NASA TN D-161

TECHNICAL NOTE

D-161

AN INVESTIGATION OF SOME ASPECTS OF THE SONIC BOOM BY MEANS OF WIND-TUNNEL MEASUREMENTS OF PRESSURES ABOUT SEVERAL BODIES AT A MACH NUMBER OF 2.01

By Harry W. Carlson

Langley Research Center
Langley Field, Va.

NATIONAL AERONAUTICS AND SPACE ADMINISTRATION

WASHINGTON

December 1959

NATIONAL AERONAUTICS AND SPACE ADMINISTRATION

TECHNICAL NOTE D-161

AN INVESTIGATION OF SOME ASPECTS OF THE SONIC BOOM BY MEANS OF WIND-TUNNEL MEASUREMENTS OF PRESSURES ABOUT SEVERAL BODIES AT A MACH NUMBER OF 2.01

By Harry W. Carlson

SUMMARY

An investigation of some aspects of the sonic boom has been made with the aid of wind-tunnel measurements of the pressure distributions about bodies of various shapes. The tests were made in the Langley 4- by 4-foot supersonic pressure tunnel at a Mach number of 2.01 and at a Reynolds number per foot of 2.5×10^6. Measurements of the pressure field were made at orifices in the surface of a boundary-layer bypass plate. The models which represented both fuselage and wing types of thickness distributions were small enough to allow measurements as far away as 8 body lengths or 64 chords. The results are compared with estimates made using existing theory.

To the first order, the boom-producing pressure rise across the bow shock is dependent on the longitudinal development of body area and not on local details. Nonaxisymmetrical shapes may be replaced by equivalent bodies of revolution to obtain satisfactory theoretical estimates of the far-field pressures.

INTRODUCTION

The "sonic boom," first recognized only as an interesting, though unexplained, physical phenomenon now poses some serious problems. With the development of new supersonic military airplanes and the possibility of supersonic transports, the previously isolated incidents may become more widespread and more severe. It is now generally understood that this annoying boom is the result of the passage over the ground of the shock formation associated with any body in supersonic flight.

A method of computing the boom-producing shock front about bodies of revolution has been developed by G. B. Whitham (ref. 1). As an

example, he has applied the method to the particular case of a parabolic body of revolution. The resulting expression for the pressure rise across the shock in the far field has often been called "the Whitham equation."

In estimating the far-field pressures about complete airplane configurations, the equivalent-body concept has proven quite useful. An exact equivalent body will be considered to be a body of revolution that produces the exact same pressure distribution in the far field as produced by a more complex nonaxisymmetrical shape. In a number of instances (refs. 2 and 3) the parabolic body treated by Whitham has been found to be a sufficiently close approximation to the exact equivalent body for complete airplanes to allow satisfactory estimates of the far-field pressures using the simple Whitham equation.

Area-rule concepts hold the promise of providing a more accurate representation of the exact equivalent body. A nonaxisymmetric configuration would have not one equivalent body, but would have a different equivalent body for each radial plane.

The effect of the lift (or weight) of the airplane on the far-field pressures has been considered by Busemann (ref. 4) and Walkden (ref. 5). There are no existing data for which the lift effects may be isolated from the thickness effects and be compared with the theory.

It is the purpose of these tests to obtain pressure measurements about several bodies for comparison with theoretical predictions using area-rule concepts. If locally produced shocks and expansions possess directional characteristics, it might be possible to provide some degree of alleviation of the boom intensity through detailed design of airplane components; this was investigated. A further purpose of these tests is that of providing data in which the lift effects may be isolated from those of thickness so that in this case too the theory may be compared directly with experiment.

The current tests were made in the Langley 4- by 4-foot supersonic pressure tunnel. At a Mach number of 2.01, measurements of the pressure field were made at orifices in the surface of a boundary-layer bypass plate. The models which represented both fuselage and wing types of thickness distributions were small enough to allow measurements as far away as 8 body lengths or 64 chords.

SYMBOLS

x,r	cylindrical coordinates of bodies of revolution or of equivalent bodies
X,R,ϕ	cylindrical coordinates of field point (see fig. 1)
l	length of equivalent bodies
d	maximum diameter of equivalent bodies
t	local wing thickness
L	characteristic dimension of model; length of bodies or root chord of wings
α	angle of attack
M	Mach number
$\beta = \sqrt{M^2 - 1}$	
p_l	local static pressure measured at the surface of the boundary-layer bypass plate
p	free-stream static pressure
$\Delta p = p_l - p$	
$\Delta p_{max} = p_l - p$	at bow shock

MODELS AND APPARATUS

The tests were conducted at a Mach number of 2.01 and at a Reynolds number per foot of 2.5×10^6 in the Langley 4- by 4-foot supersonic pressure tunnel. The models were sting mounted on a remotely controlled support system which provided both lateral and longitudinal motion as well as roll-angle variation. (See fig. 1.) Measurements of the pressure field were made at orifices in the surface of a stationary boundary-layer bypass plate (also shown in fig. 1). Calibrated Statham gages having ranges of $\frac{1}{2}$ and 1 lb/sq in. and an accuracy of 1 percent were used.

Sketches of the test models are shown in figure 2. Model A is an elliptical body of revolution intended to represent a fuselage type of thickness distribution. Model C is a low-aspect-ratio wing having a parabolic-arc section given by the accompanying equation. Model B has a special shape designed to produce a compression in one direction and an expansion in another. This model was used to investigate the possibility of reducing the boom intensity by aerodynamic means. Each of these first three models had the same distribution of normal cross-sectional area. According to the transonic area rule each would have the same transonic drag rise. Model D is a parabolic body of revolution having the same length and maximum cross-sectional area as each of the first three bodies.

Models E and F (wedge-section wings of aspect ratio 2) were tested through an angle-of-attack range so that by subtraction the pressures due to lift could be obtained. The wing angle of attack was varied by bending the sting. Two models were used in order to cover a large range of separation distances R/L; model F was one-fourth the size of model E.

An added configuration used in these tests was the airplane model (model G) shown in figure 3. This configuration was designed to be representative of future transport airplanes.

Since supersonic-area-rule concepts will be used later in the report, figure 4 has been prepared to show $M = 2.01$ equivalent bodies for some of the models.

RESULTS AND DISCUSSION

Basic Data

The measured flow-field data from these tests are shown in figures 5 to 11. Static pressures at the surface of the boundary-layer bypass plate have been plotted as a function of streamwise distance behind the Mach cone from the model nose or leading edge. On each page, data are shown for four separation distances of model and plate. If it can be assumed that the plate acts as a perfect reflection plane the measured pressures are exactly twice those that would exist in the absence of a plate. Since the plate is quite flat and smooth, the factor of two is expected to hold.

Since small variations in tunnel Mach number can cause relatively large shifts in the location of the shock front when referenced to the length of these small models, the longitudinal location of the pressure signature should not be used quantitatively. From static calibrations and checks of repeatability, the accuracy of the measured pressure

ratios $\Delta p/p$ is estimated to be ± 0.005. Because of the additional difficulty of establishing maximum values, the pressure rise at the bow shock is estimated to be accurate within ± 10 percent or ± 0.005 whichever is greater.

For models A to D (figs. 5 to 8) differences in the pressure traces are evident at the close-in positions. At 8 body lengths, however, remarkably similar curves are shown. In each case an abrupt pressure rise is followed by a linear decline to an equal value of negative pressure after which a recompression to nearly the free-stream value occurs. (Pressure distributions of this type are often referred to as N-curves.) The so-called far field will be assumed to begin at the separation distance where this condition is reached.

Thickness-Induced Pressures

The attenuation of pressures with distance can best be shown in the form of plots of the pressure rise at the bow shock against distance. Figure 12 contains such a plot for three orientations of model B, the "hatchet-shaped" body. Notice that for the lower curve, the surface of the model facing the plate is inclined so as to produce an expansion in the direction of the orifice. It was hoped that such a fuselage configuration would provide some alleviation of the shock intensity by producing an expansion to continue out into the field and cancel a compression from some other source. However, even at the closest measuring point a positive value rather than a negative value of $\Delta p/p$ was recorded. Aside from that, the important point of this figure deals not with any one curve but with the trend to a common value of pressure and axial symmetry of flow at the larger distances. Data are also shown for model A which, it should be recalled, has the same longitudinal area distribution. The pressures measured for model A agree fairly well with those for model B, indicating that to the first order the pressure rise in the far field is dependent on the development of body area and not on local details.

A plot similar to the previous one has been prepared for model C (fig. 13). Here the trend to axial symmetry is not as evident. In fact, it is reasonable to believe that axial symmetry may not be achieved at any distance for the wing-shaped body. From these data and those of the previous figure, it appears that, while they are dependent to a large degree on the normal area distribution, the far-field conditions are also sensitive to radial position for bodies that depart greatly from axial symmetry. This will be discussed more fully after the introduction of a theoretical method of treating the problem.

A method of predicting the pressure rise at the bow shock emanating from bodies of revolution has been developed by G. B. Whitham in

reference 1. When applied in particular to a parabolic body of revolution the equation becomes

$$\frac{\Delta p_{max}}{p} = K_1 K_2 \beta^{1/4} \frac{d/l}{(R/l)^{3/4}} \qquad (1)$$

where K_1 is a reflection constant, in this case assumed to be 2.0. Randall, in reference 6, showed that for a parabolic body of revolution the body-shape constant K_2 should be 0.64 as used herein instead of 0.53 as originally given by Whitham. For a general body of revolution the pressure can be approximated by letting the body-shape constant be a variable which depends to a large degree on the location of the maximum diameter. The equation as shown above may be used to approximate the pressure rise in the far field for a wide range of body shapes (even complete airplanes) when d/l is for the appropriate equivalent body of revolution. It has been shown in several instances that a reasonably accurate equivalent body is determined by the distribution of normal cross-sectional area (the supersonic-area-rule equivalent body for the limiting case of $M = 1.0$).

In figure 14 the theory is compared with data measured for model A, (the transonic-equivalent body for models B and C) and with model D which is a parabolic body of revolution of the same fineness ratio, corresponding exactly to the mathematical model used in the theory. The theory is shown to closely approximate the variation of pressure rise with distance but to overestimate the measurement by about 25 percent. The close agreement between the measured data for the two bodies shows that the lack of agreement with theory is not due to the parabolic-body approximation. It must be remembered that the theory is based on slender-body approximations and that these fineness-ratio-5 bodies are not really slender. In addition it should be noted that the experimental accuracy in the pressure rise is not much better than 10 percent and that the reflection constant of 2.0 used in the theory is an upper limit. This may be at least partially the cause of those discrepancies shown.

Since in the application of the Whitham equation (eq. (1)) the d/l term represents an equivalent body of revolution some question remains as to how the body is obtained for shapes that depart greatly from axial symmetry. As was suggested before, the ideas incorporated in the supersonic area rule may find application here. For the wing-shaped body, model C (which as shown in fig. 15 did not have an axisymmetrical flow field at 8 body lengths), the equivalent body was found in the following manner. For a given arbitrary point in space, visualize a plane containing that point and the axis of the body (ϕ = Constant). Now consider a Mach cone originating at the body nose and centered on the body axis. The plane and the cone intersected in

a straight line. A second plane, called the "cutting plane," is defined as a plane tangent to the Mach cone at this line. The equivalent body for this field location is defined by the frontal projection of the areas intercepted by the "cutting plane" as the Mach cone apex advances along the body axis. The far-field pressures may be approximated by using in the Whitham equation (eq. (1)) the fineness ratio of a parabolic body of revolution having the same length and maximum area.

Far-field pressures determined in the previously described manner have been compared with experimental data in figure 15. The pressure rise across the shock at 8 body lengths has been plotted against radial position ϕ. As before, the theory overestimates the measurements but gives the trend reasonably well. From figure 4 showing the area distribution at $\phi = 0^\circ$ and at $\phi = 90^\circ$ it can be seen that a large change in equivalent body fineness ratio is responsible for a relatively small change in far-field pressures. The nondimensional distance R/L (used in fig. 15) is based on the length of the real body not the equivalent body. Thus, qualitatively and to some degree quantitatively it can be shown that at this Mach number the equivalent body depends on the radial position of the field point; this is probably true at all supersonic Mach numbers. Walkden, in reference 5, has developed a method of estimating the far-field pressures about wing-body combinations which incorporates these considerations and in addition treats the wing-body interference.

Lift-Induced Pressures

When a wing is placed at an angle of attack with respect to the free stream, pressures greater than those due to thickness alone are created on the underside. On the upper surface, however, correspondingly lower pressures exist so that on the average the body produces no greater pressure rise across the shock than before. The important question is this: Will the increased pressure rise across the shock below the wing propagate out into the far field in the same manner as thickness-induced pressures or will an interaction of the flows below and above the wing produce a canceling effect? The wing-tip vortex produces a mechanism for such interaction.

Two theoretical methods of estimating lift-induced pressures are those of Busemann (ref. 5) and of Walkden (ref. 4). In applying both methods it is necessary to compute separately the pressure due to thickness alone and the pressure due to the combined effects of thickness and lift. The increment due to lift is then found by subtraction. In figure 16 incremental far-field pressures due to an angle of attack of 5° for models E and F have been plotted against separation distance expressed in chords. The theory (both methods) shows reasonable agreement with the experimental data. The reason for the discrepancy

between the experimental data for models E and F is not fully known. Model F was extremely small and it was difficult to determine the wedge angle and to set the angle of attack accurately. In addition, because of the small sting size, there was considerable vibration of this model during the tests which may have affected the results.

The variation of far-field pressure with angle of attack can be seen in figure 17. For a separation distance of 16 chords, the pressure rise across the bow shock from models E and F has been plotted as a function of angle of attack. The theory of Walkden including both thickness and lift effects is shown as a solid line. The theory shows the trend very well.

In figure 18 the ratio of the lift-induced pressures at $\alpha = 5^{\circ}$ to the thickness-induced pressures is plotted against separation distance. Close to the model, the lift and thickness effects are nearly equal and the ratio is close to one. However in this region the lift-induced pressures attenuate more rapidly and the ratio decreases until a distance of about 16 chords is reached. Beyond that point the ratio remains constant at about 0.45. This is consistent with the theory (ref. 5) which gives the same far-field rate of attenuation for lift-induced pressures as for thickness-induced pressures. Thus it seems that there is only a limited region near the lifting body in which an interaction between the upper and lower portions of the flow takes place.

It can be shown (see ref. 4) that for supersonic airplanes flying at high altitudes the lift-induced far-field pressures would theoretically be equal to or larger than the thickness-induced pressures. Unfortunately, the data for the airplane model of these tests (fig. 11) showed that the far-field conditions had not been reached. Therefore, no analysis was attempted. In this regard, mention should be made of the tests of reference 2 where pressures were measured below and to the side of a jet fighter flying at 35,000 feet at a Mach number of 1.05. In this case too, the pressure signatures did not show clearly the complete attainment of the far-field N-curve. Perhaps for some configurations the far-field conditions may exist only at extreme distances. It has been noted that lift effects may be neglected in correlating measured ground pressures during full-scale tests with the theory. (See ref. 3.) Obviously, the lift effects are as yet not well understood.

CONCLUDING REMARKS

An analysis of wind-tunnel measurements of pressure fields about bodies of various shapes provides the following conclusions:

To the first order the pressure rise across the bow shock in the far field is dependent on the normal cross-sectional area distribution and not on local details. Nonaxisymmetrical shapes may be replaced by equivalent bodies of revolution in estimating far-field pressures. It has been shown qualitatively and to some degree quantitatively that at a Mach number of 2.01, the equivalent body depends on the radial position of the field point. This is probably true at all supersonic Mach numbers. Existing theoretical methods gave an adequate estimation of the magnitude of the thickness-induced far-field pressure rise across the bow shock and gave very well the rate of attenuation with distance. Near a wing, lift-induced pressures attenuate at a more rapid rate than thickness-induced pressures. However it appears that in the far field lift-induced pressures attenuate at the same rate as the thickness pressures. Theoretical estimates of the lift-induced pressures showed useful correlation with the measured data.

Langley Research Center,
National Aeronautics and Space Administration,
Langley Field, Va., August 18, 1959.

REFERENCES

1. Whitham, G. B.: The Flow Pattern of a Supersonic Projectile. Communications on Pure and Appl. Math., vol. V, no. 3, Aug. 1952, pp. 301-348.

2. Mullens, Marshall E.: A Flight Test Investigation of the Sonic Boom. AFFTC-TN-56-20, Air Res. and Dev. Command, U.S. Air Force, May 1956.

3. Maglieri, Domenic J., and Carlson, Harry W.: The Shock-Wave Noise Problem of Supersonic Aircraft in Steady Flight. NASA MEMO 3-4-59L, 1959.

4. Busemann, Adolf: The Relation Between Minimizing Drag and Noise at Supersonic Speeds. Proc. Conf. on High-Speed Aeronautics, Antonio Ferri, Nicholas J. Hoff, and Paul A. Libby, eds., Polytechnic Inst. of Brooklyn, c.1955, pp. 133-144.

5. Walkden, F.: The Shock Pattern of a Wing-Body Combination, Far From the Flight Path. Aero. Quarterly, vol. IX, p.2, May 1958, pp. 164-194.

6. Randall, D. G.: Methods for Estimating Distributions and Intensities for Sonic Bangs. Tech. Note No. Aero 2524, British R.A.E., Aug. 1957.

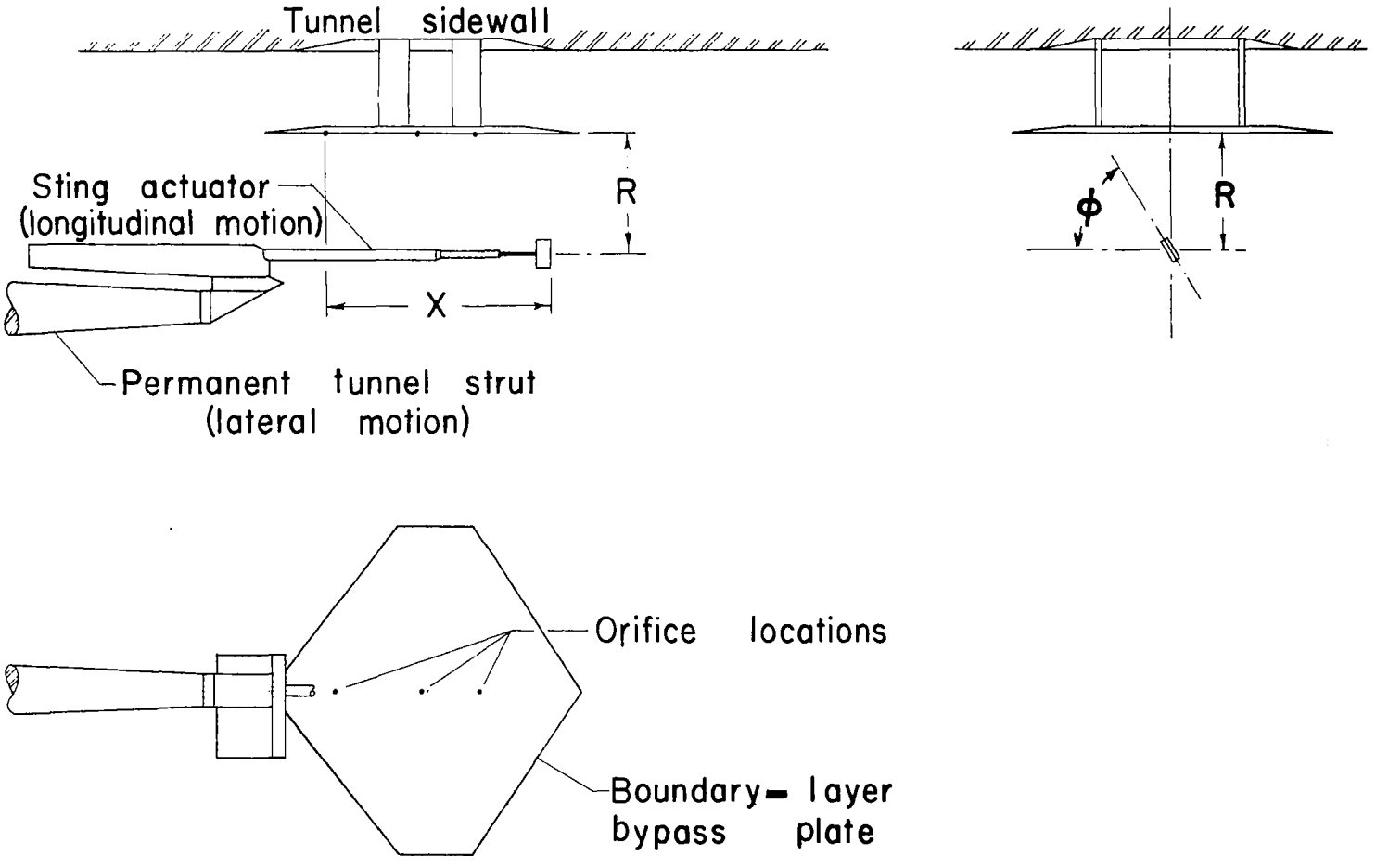

Figure 1.- Sketches of test setup.

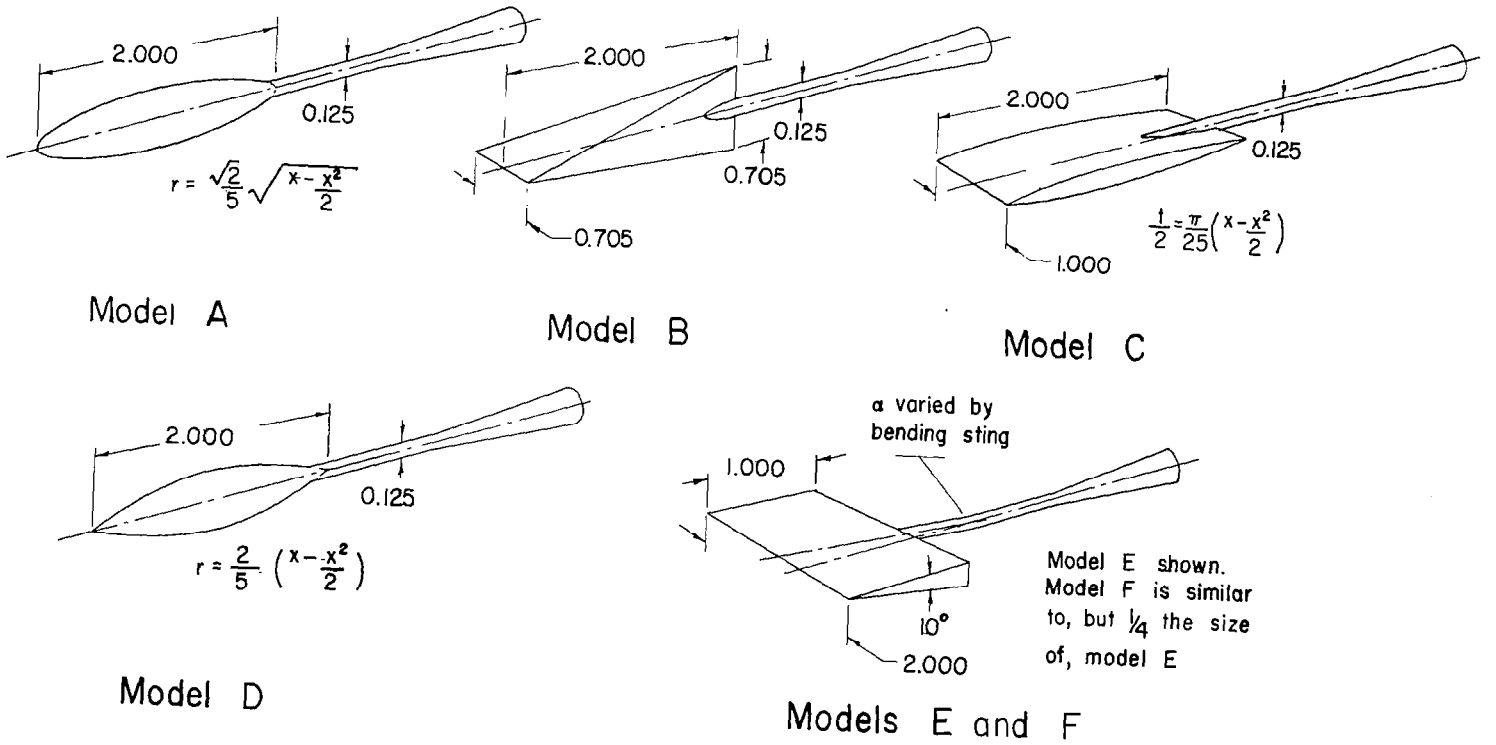

Figure 2.- Sketches of test models A to F. All dimensions are in inches. Models shown in the $\phi = 0^{\circ}$ position.

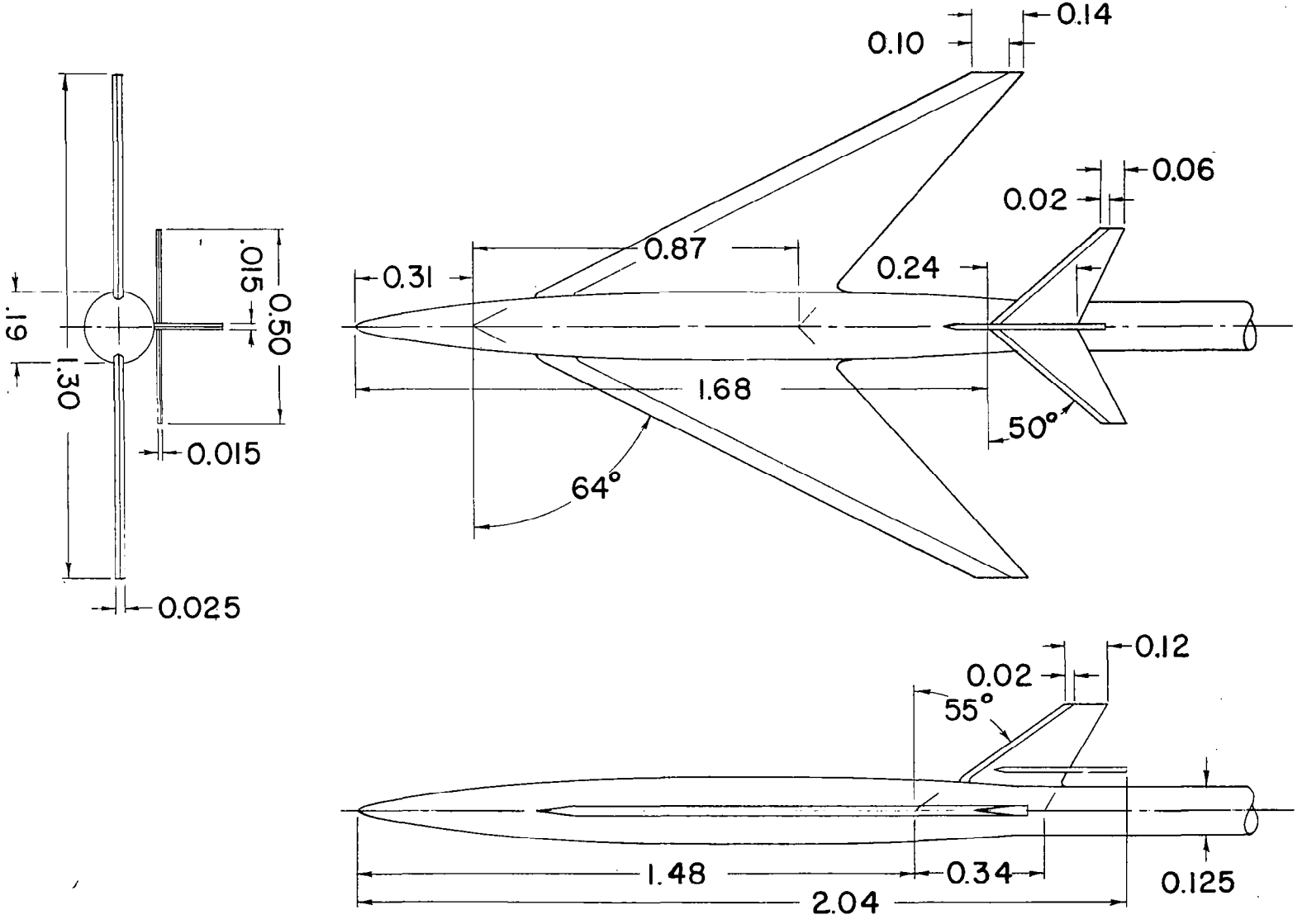

Figure 3.- Sketch of test model G. All dimensions are in inches.

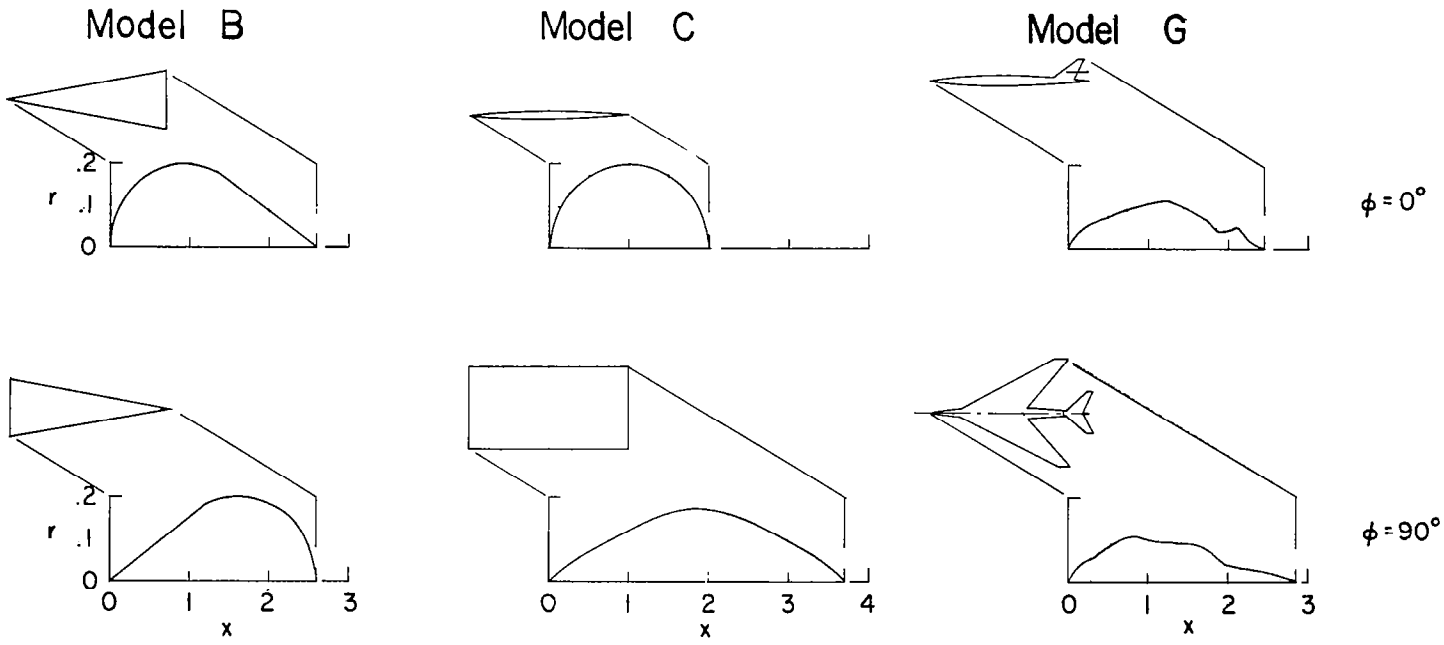

Figure 4.- Equivalent bodies of revolution for several of the models according to the supersonic-area-rule concept. M = 2.01. All dimensions are in inches.

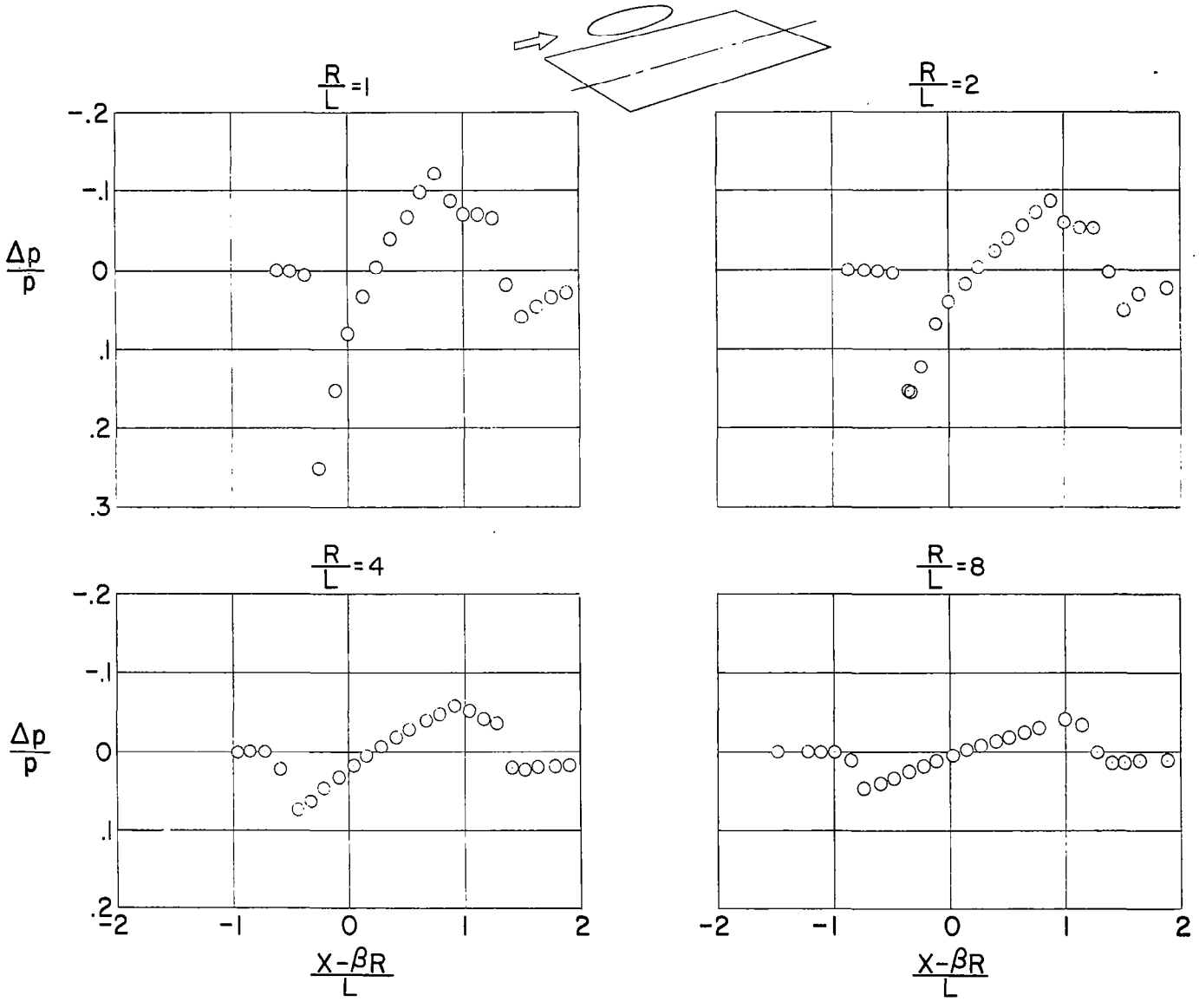

Figure 5.- Pressure ratio measured on the surface of the boundary-layer bypass plate. Model A.

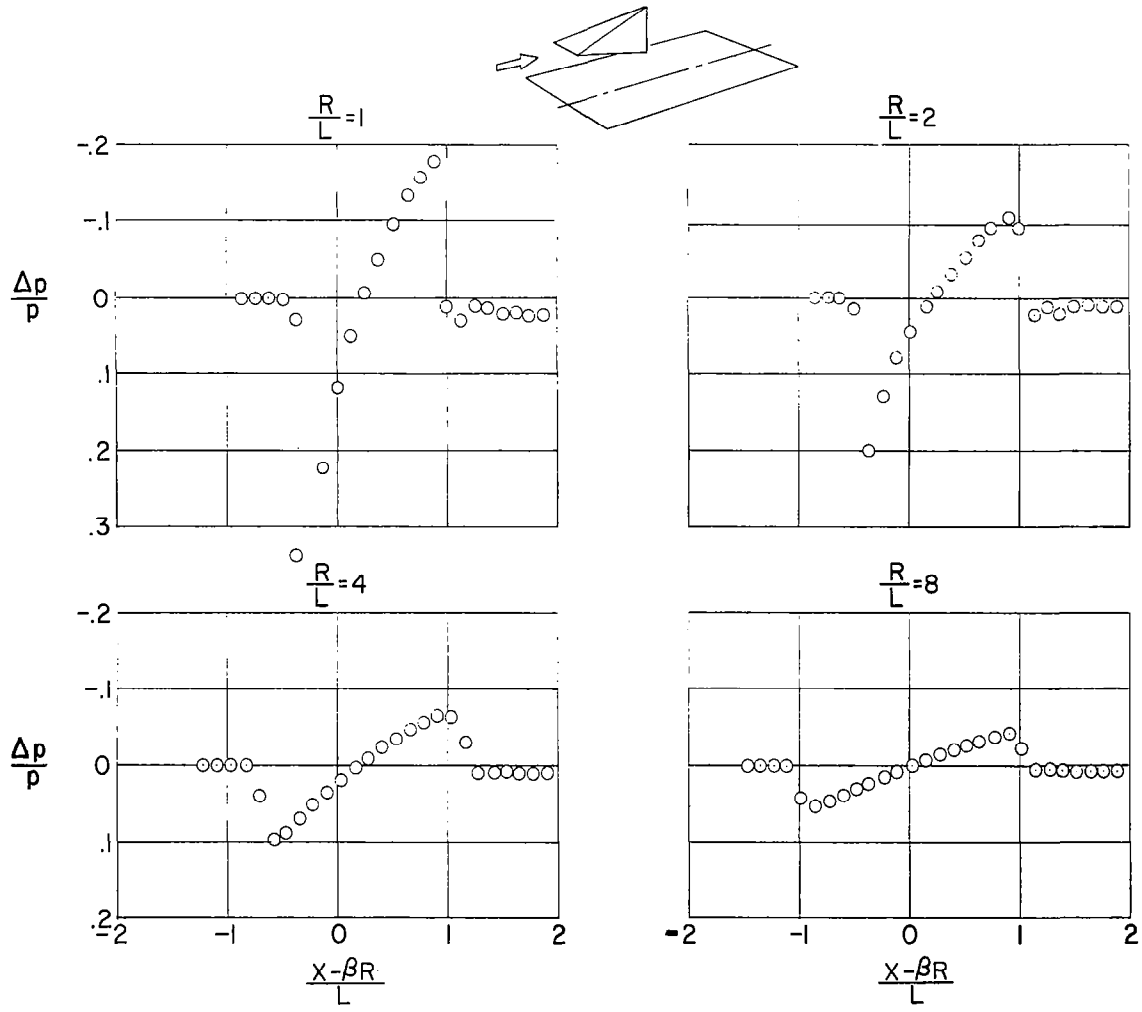

(a) $\phi = 0^{\circ}$.

Figure 6.- Pressure ratio measured on the surface of the boundary-layer bypass plate. Model B.

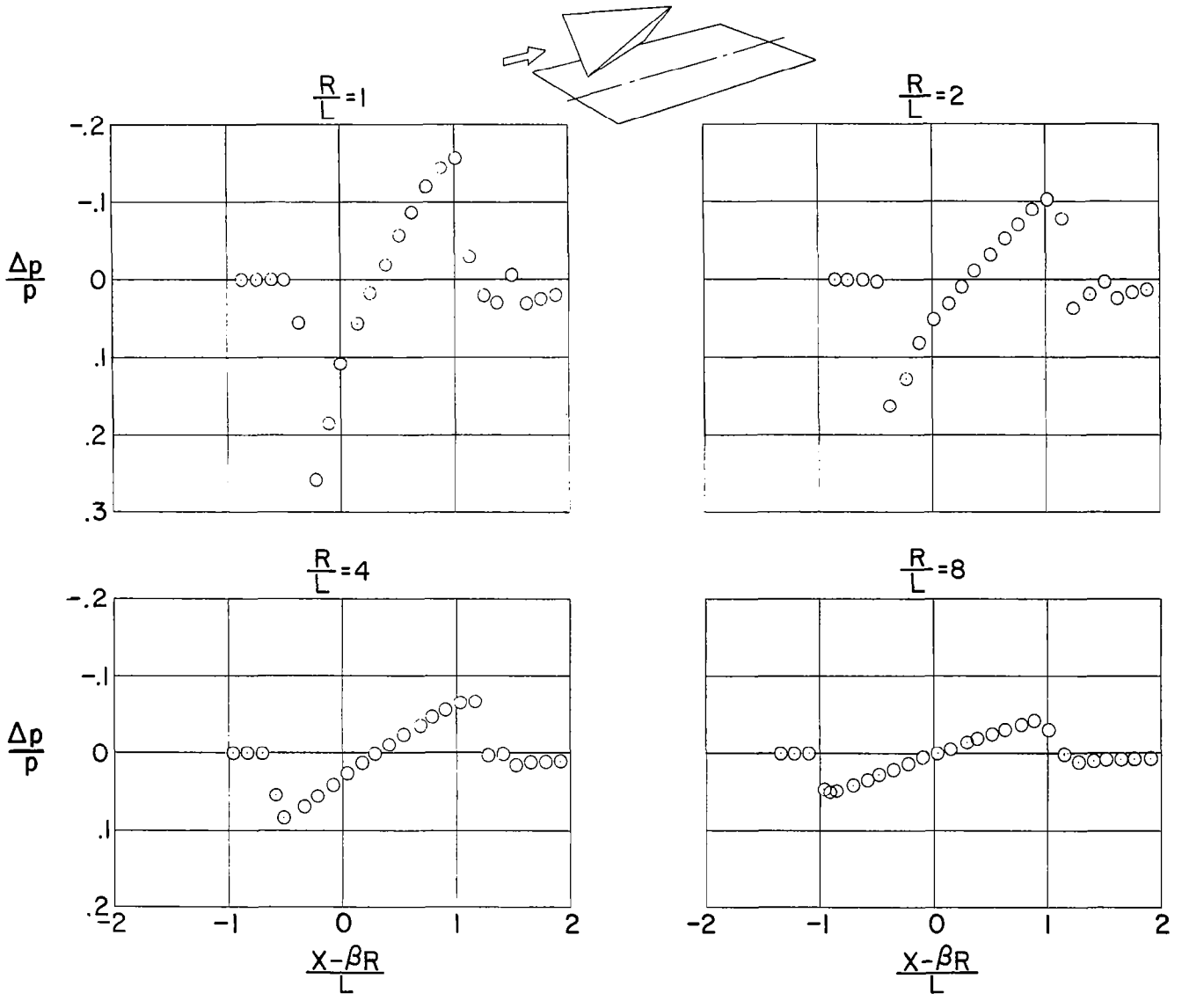

(b) $\phi = 45°$.

Figure 6.- Continued.

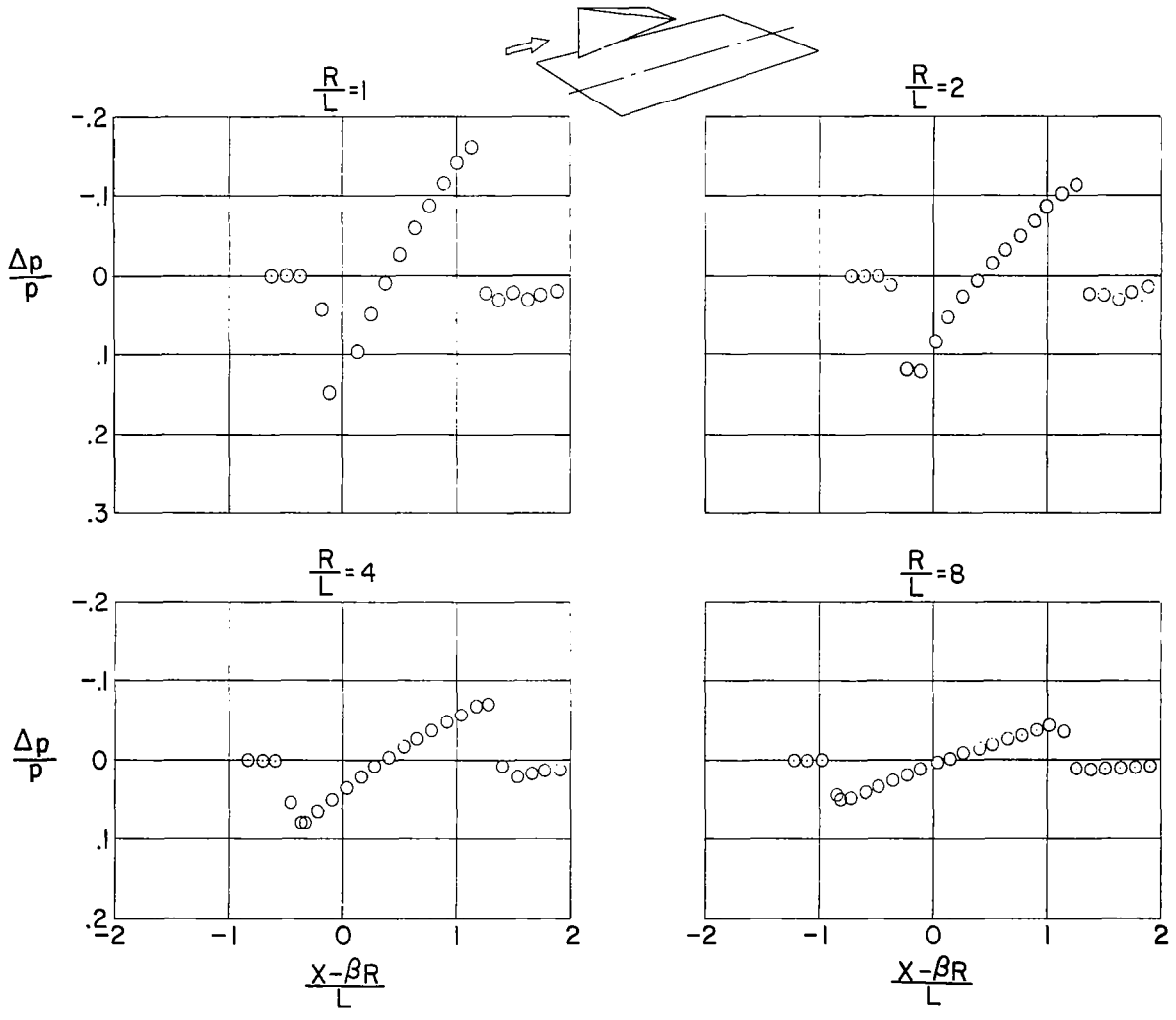

(c) $\phi = 90^{\circ}$.

Figure 6.- Concluded.

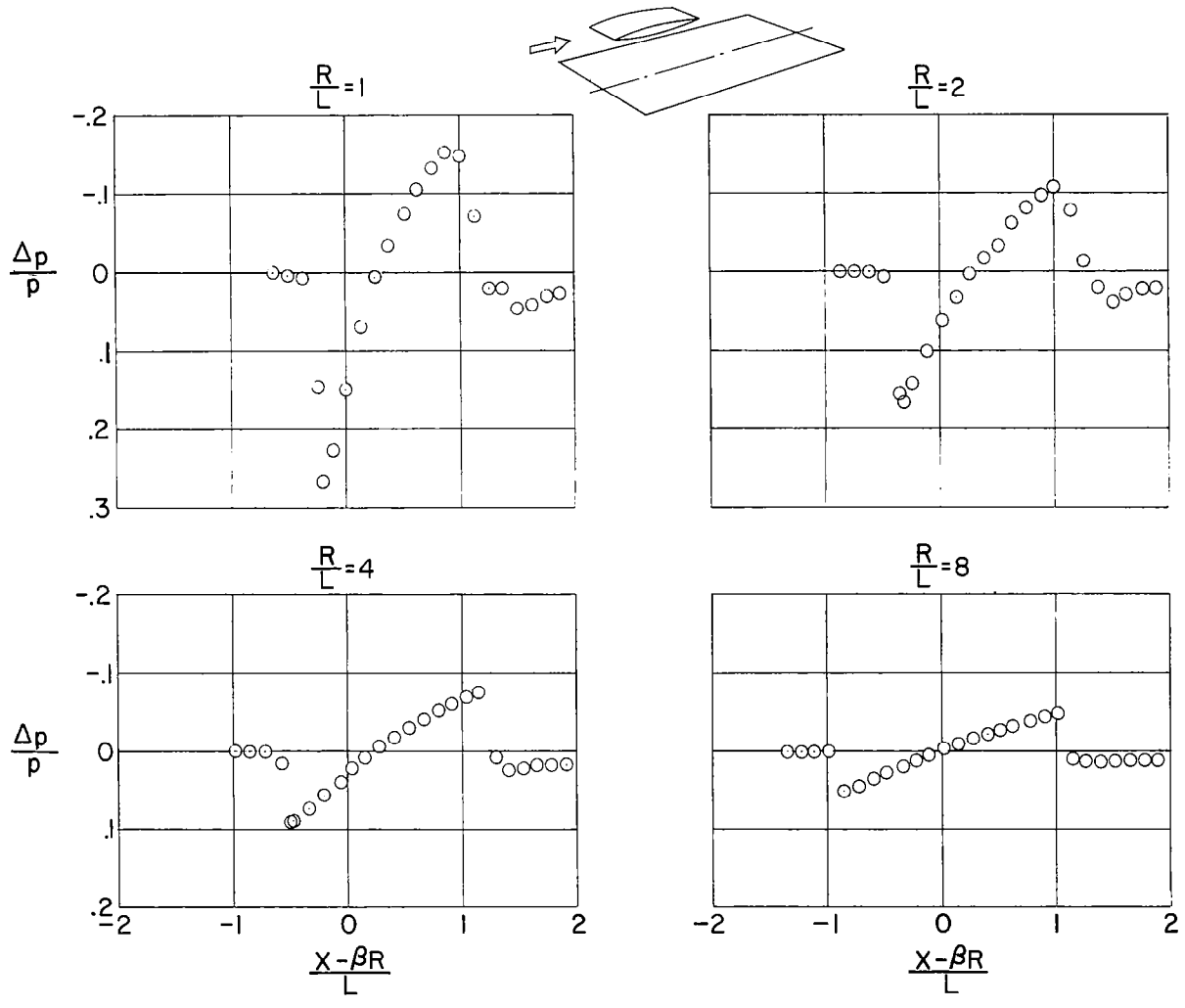

(a) $\phi = 0^{\circ}$.

Figure 7.- Pressure ratio measured on the surface of the boundary-layer bypass plate. Model C.

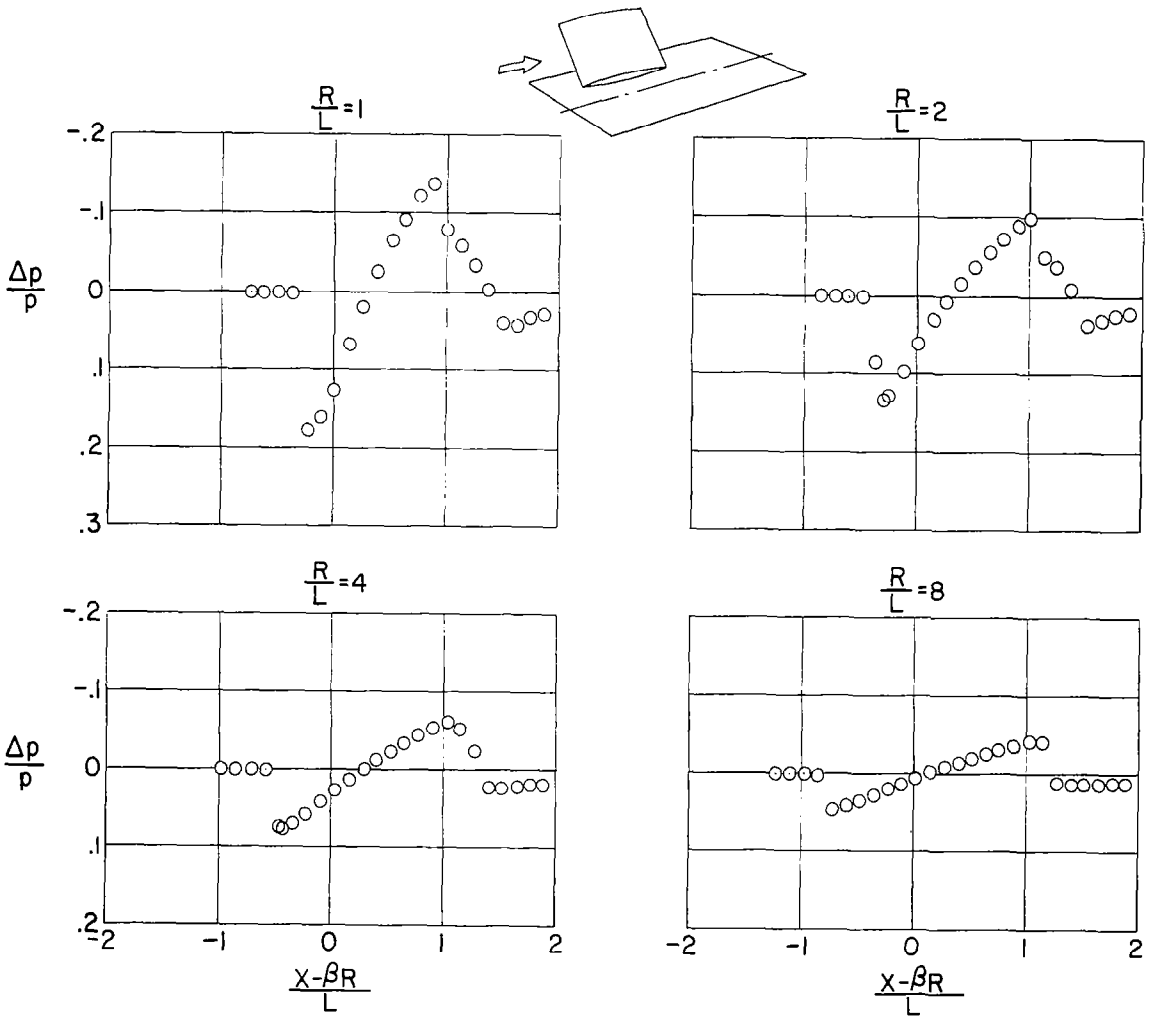

(b) $\phi = 45^{\circ}$.

Figure 7.- Continued.

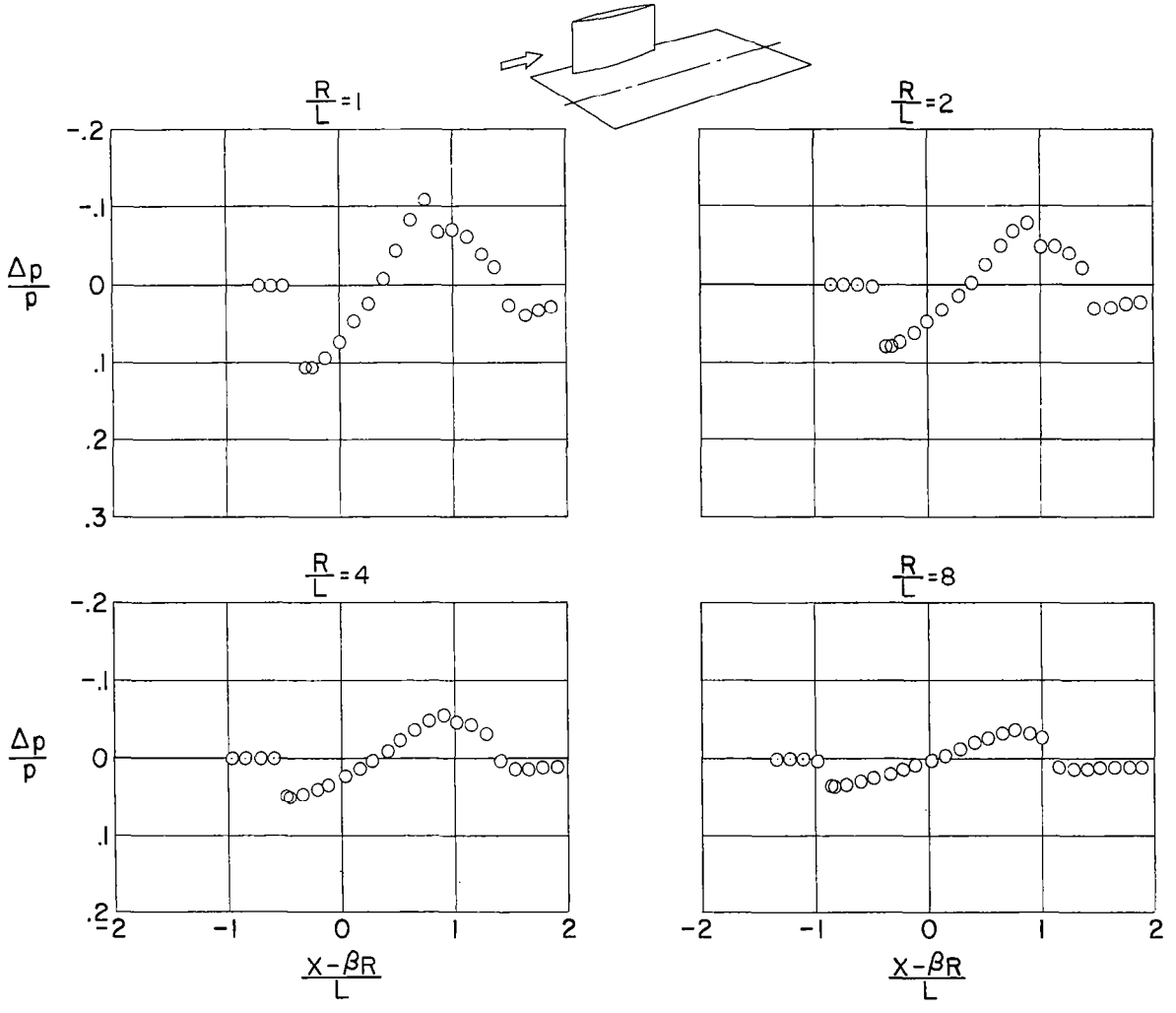

(c) $\phi = 90^{\circ}$.

Figure 7.- Concluded.

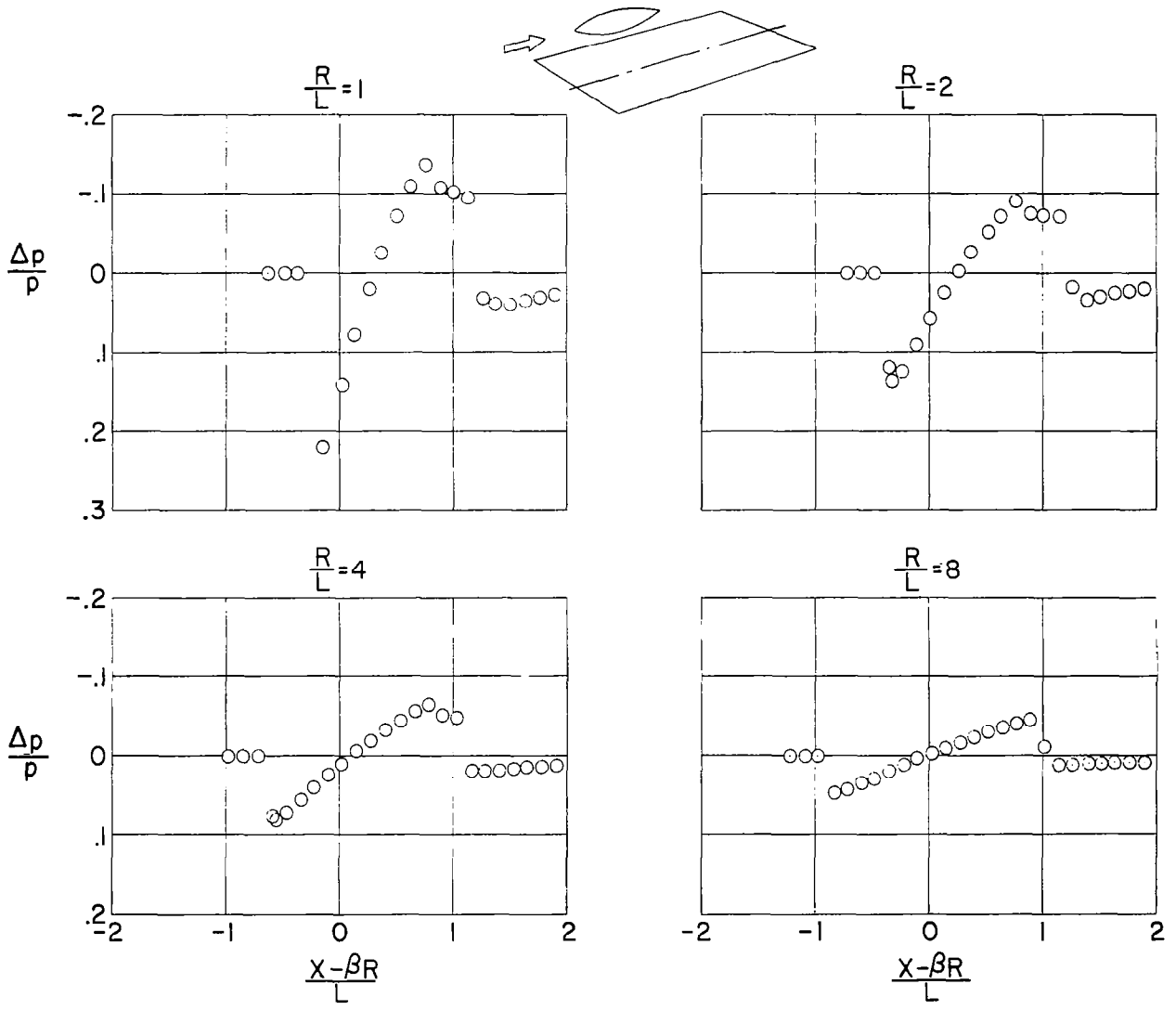

Figure 8.- Pressure ratio measured on the surface of the boundary-layer bypass plate. Model D.

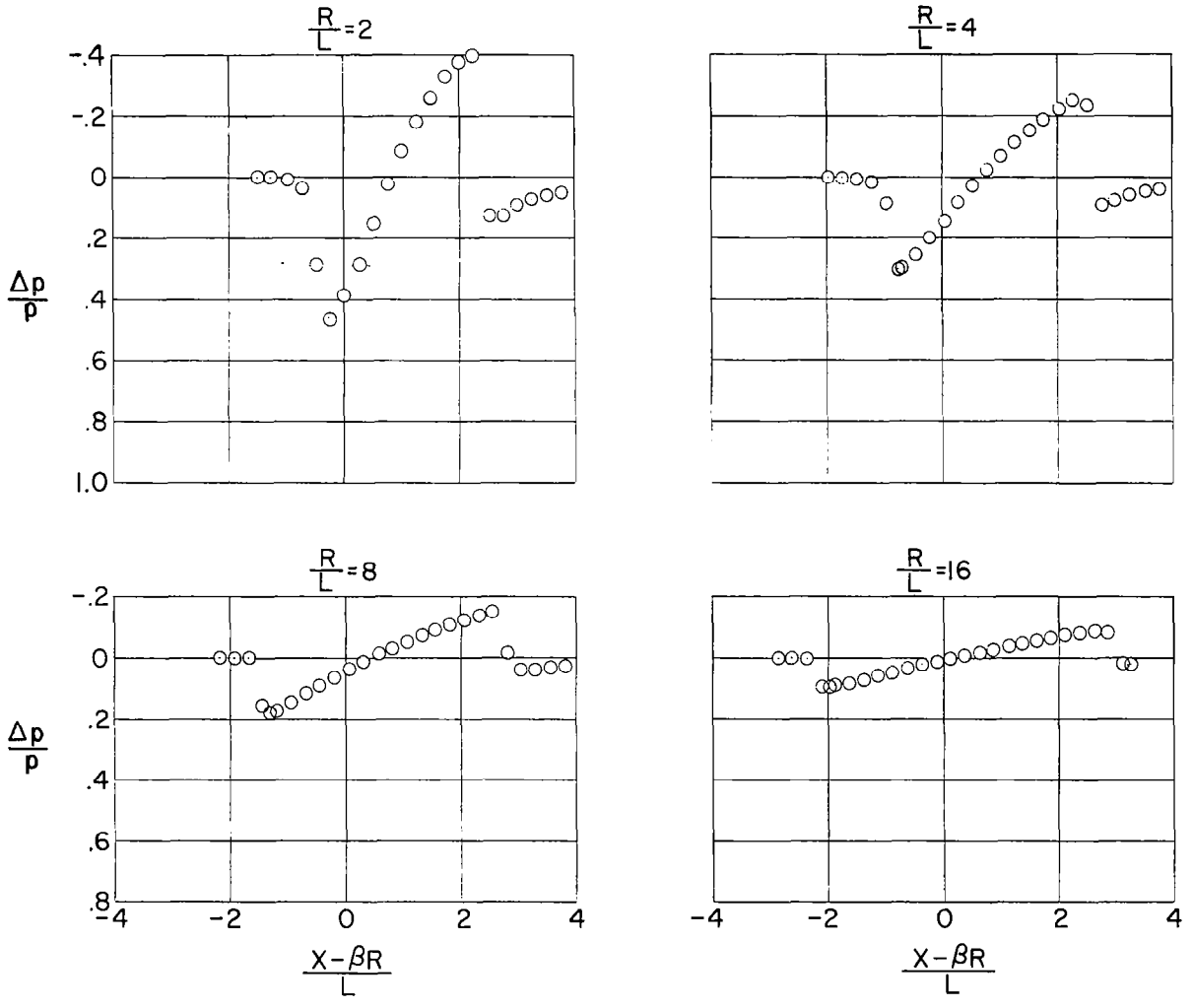

(a) $\alpha = 0^{\circ}$; $\phi = 0^{\circ}$.

Figure 9.- Pressure ratio measured on the surface of the boundary-layer bypass plate. Model E.

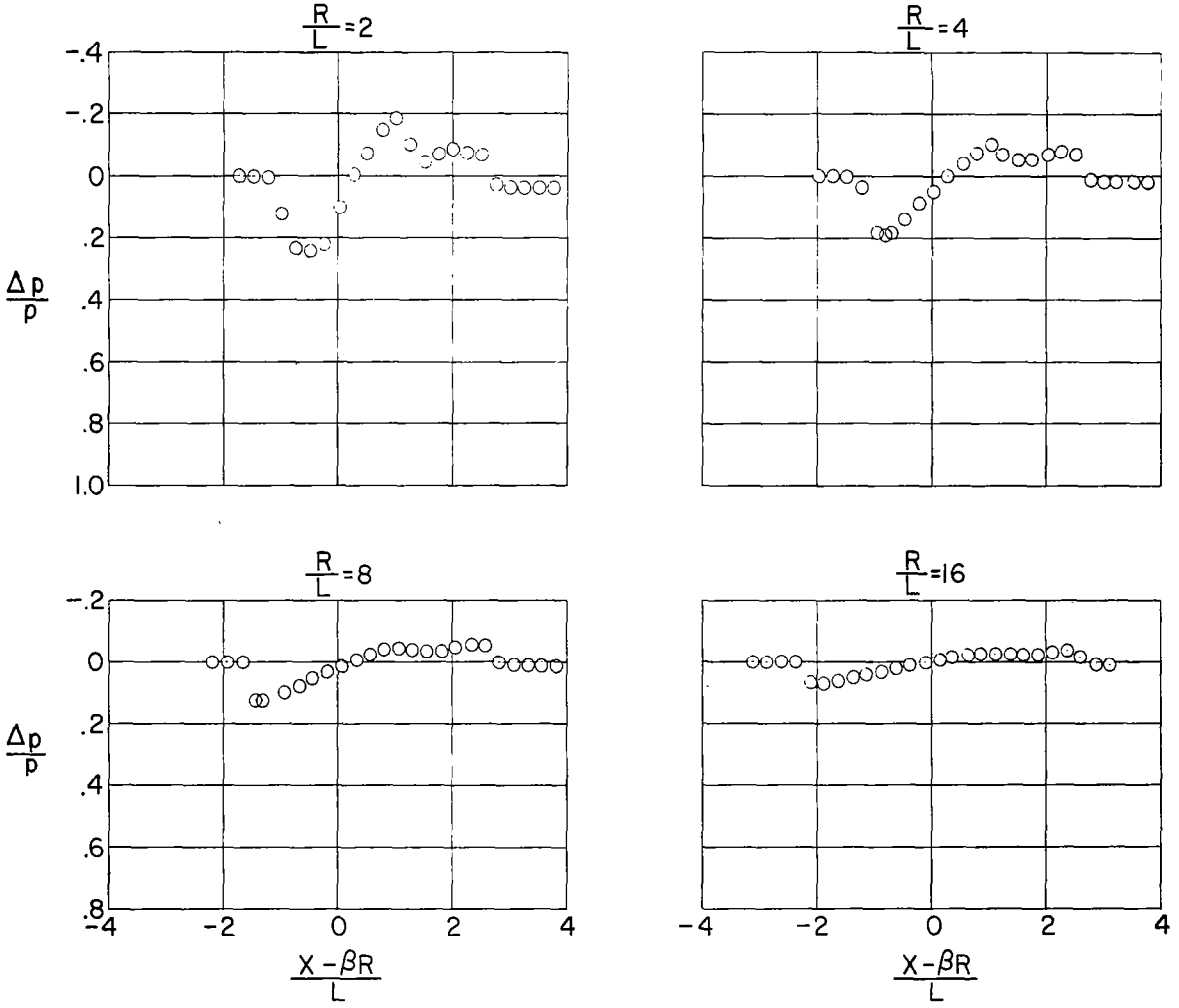

(b) $\alpha = 0^{\circ}$; $\phi = 45^{\circ}$.

Figure 9.- Continued.

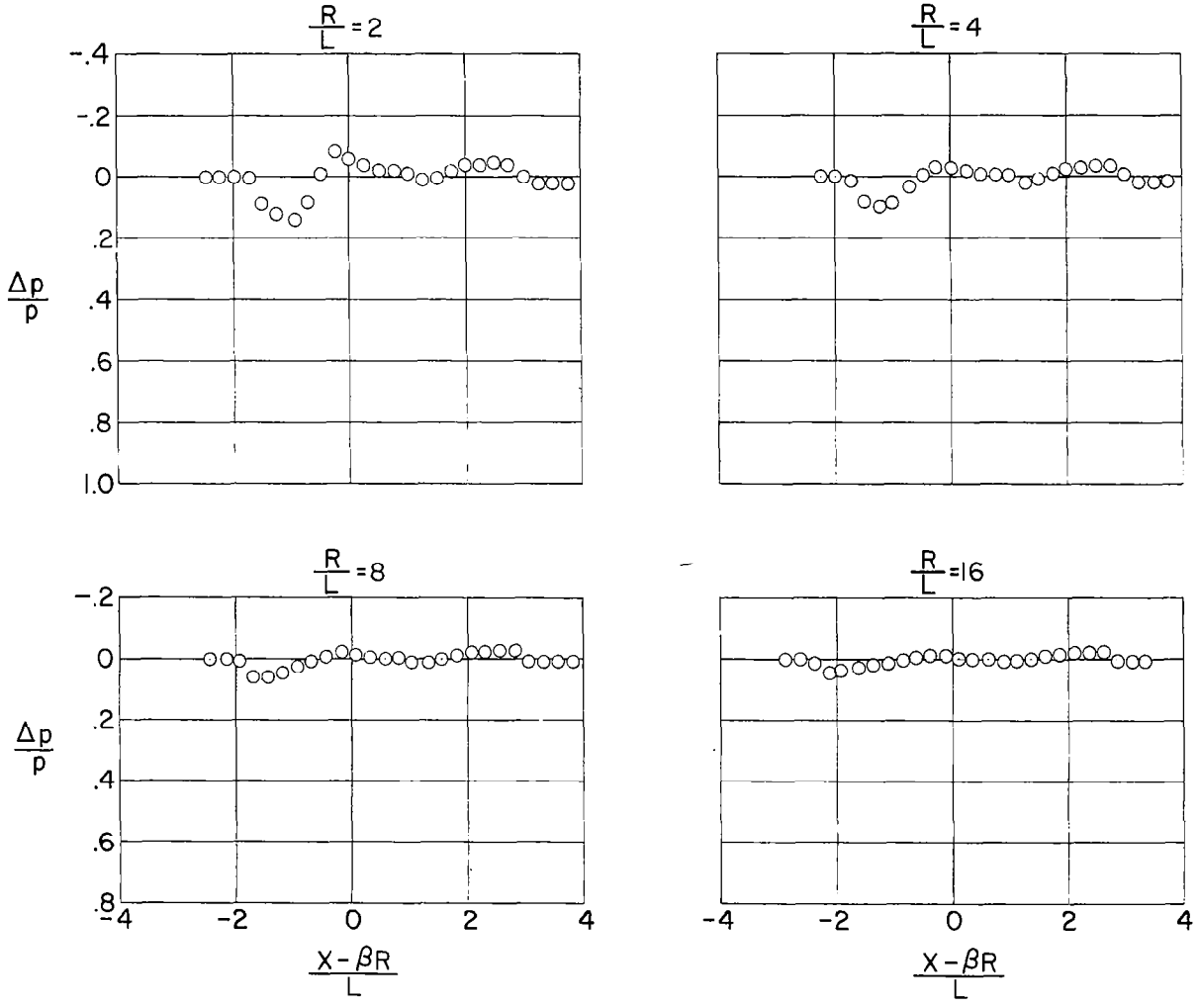

(c) $\alpha = 0^{\circ}$; $\phi = 90^{\circ}$.

Figure 9.- Continued.

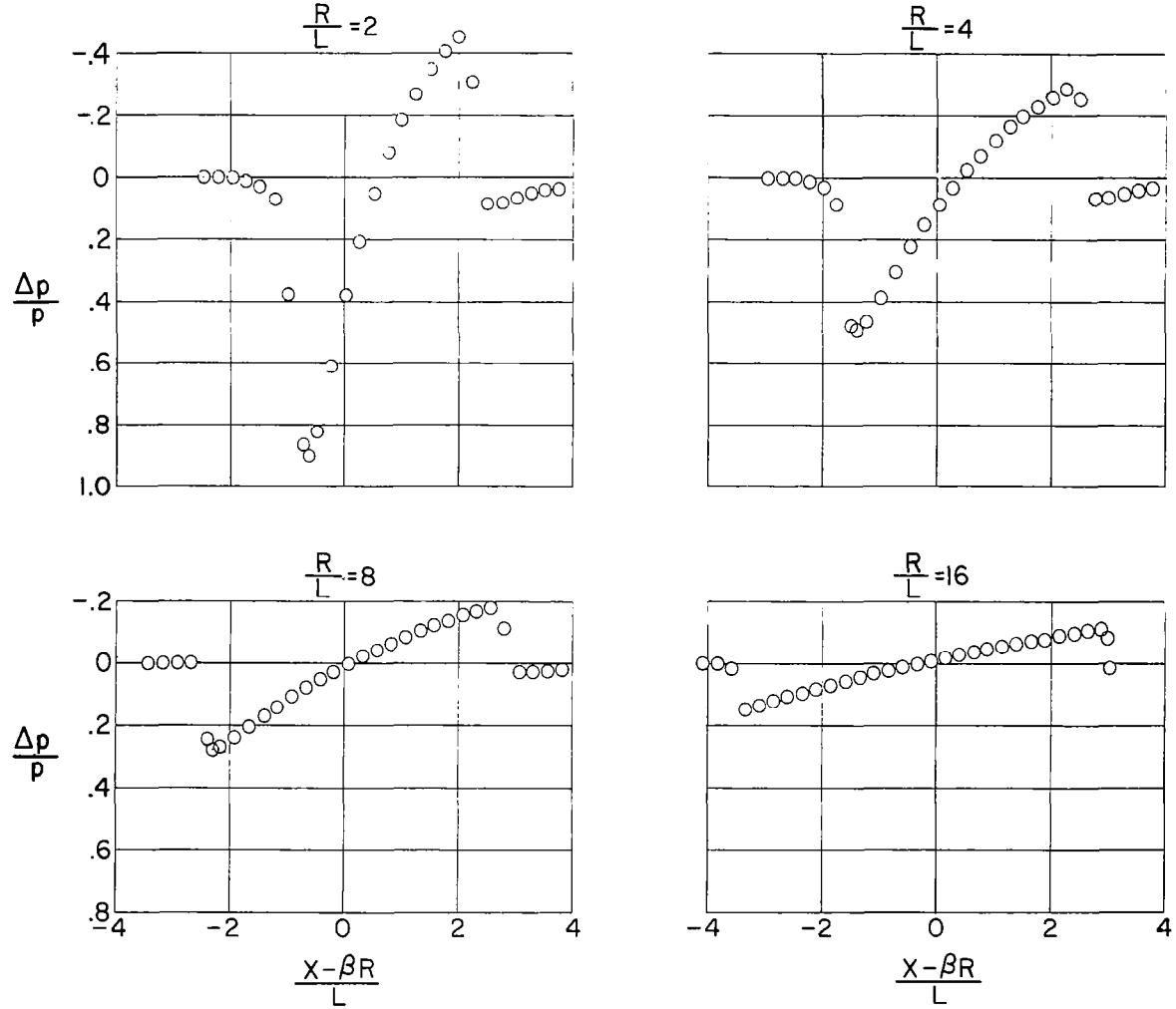

(d) $\alpha = 5^{\circ}$; $\phi = 0^{\circ}$.

Figure 9.- Continued.

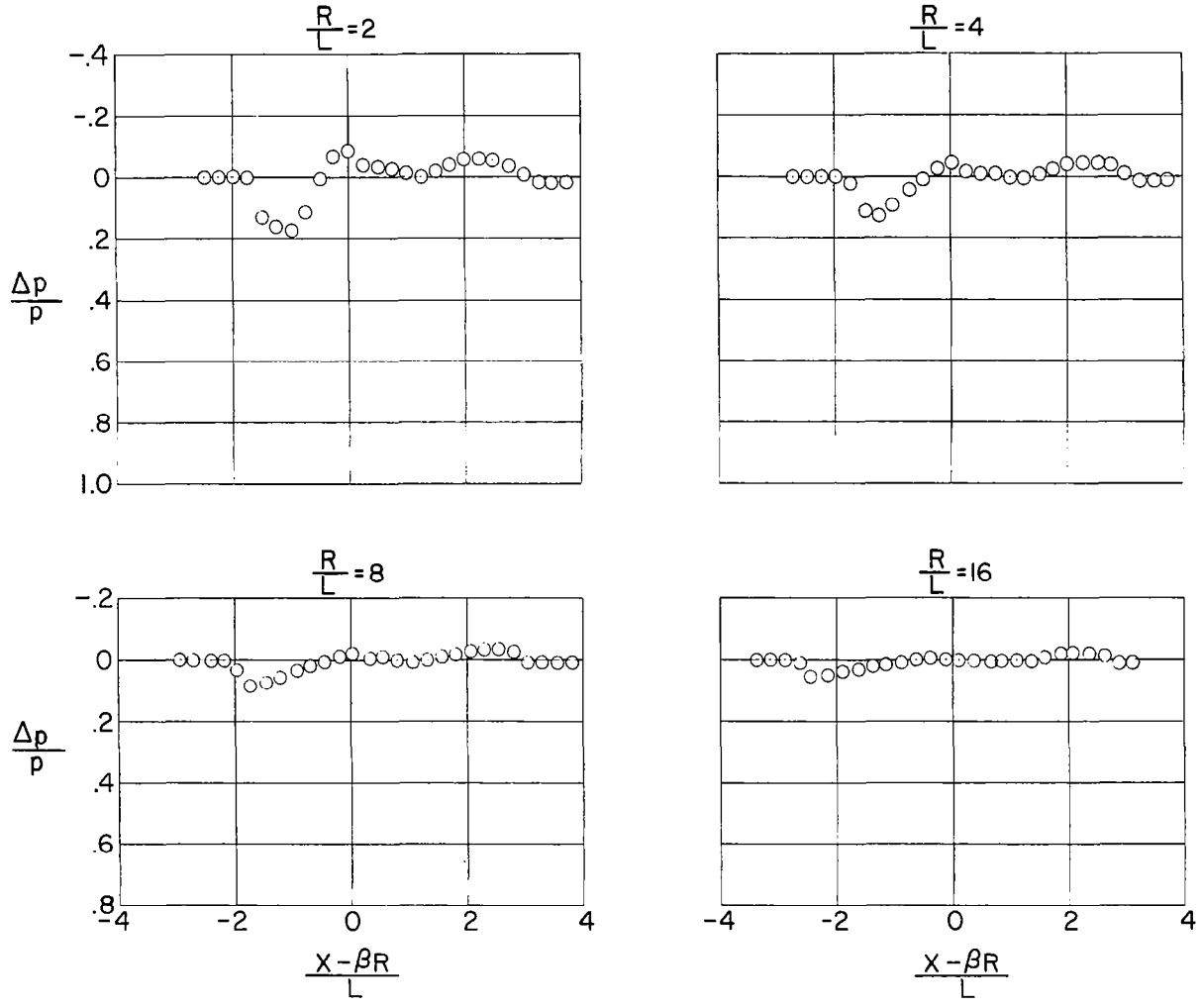

(e) $\alpha = 5^{\circ}$; $\phi = 90^{\circ}$.

Figure 9.- Continued.

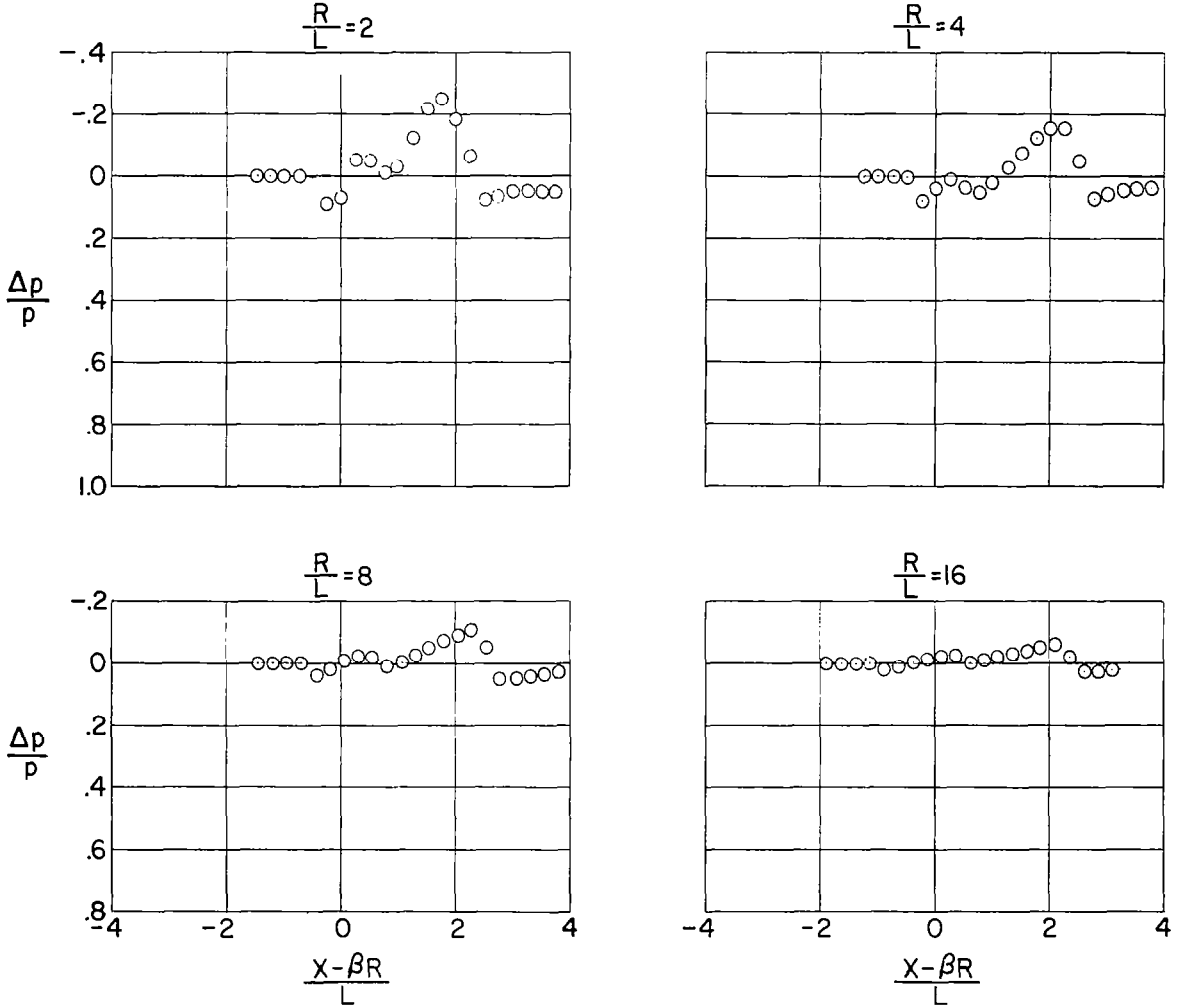

(f) $\alpha = 5^{\circ}$; $\phi = 180^{\circ}$.

Figure 9.- Continued.

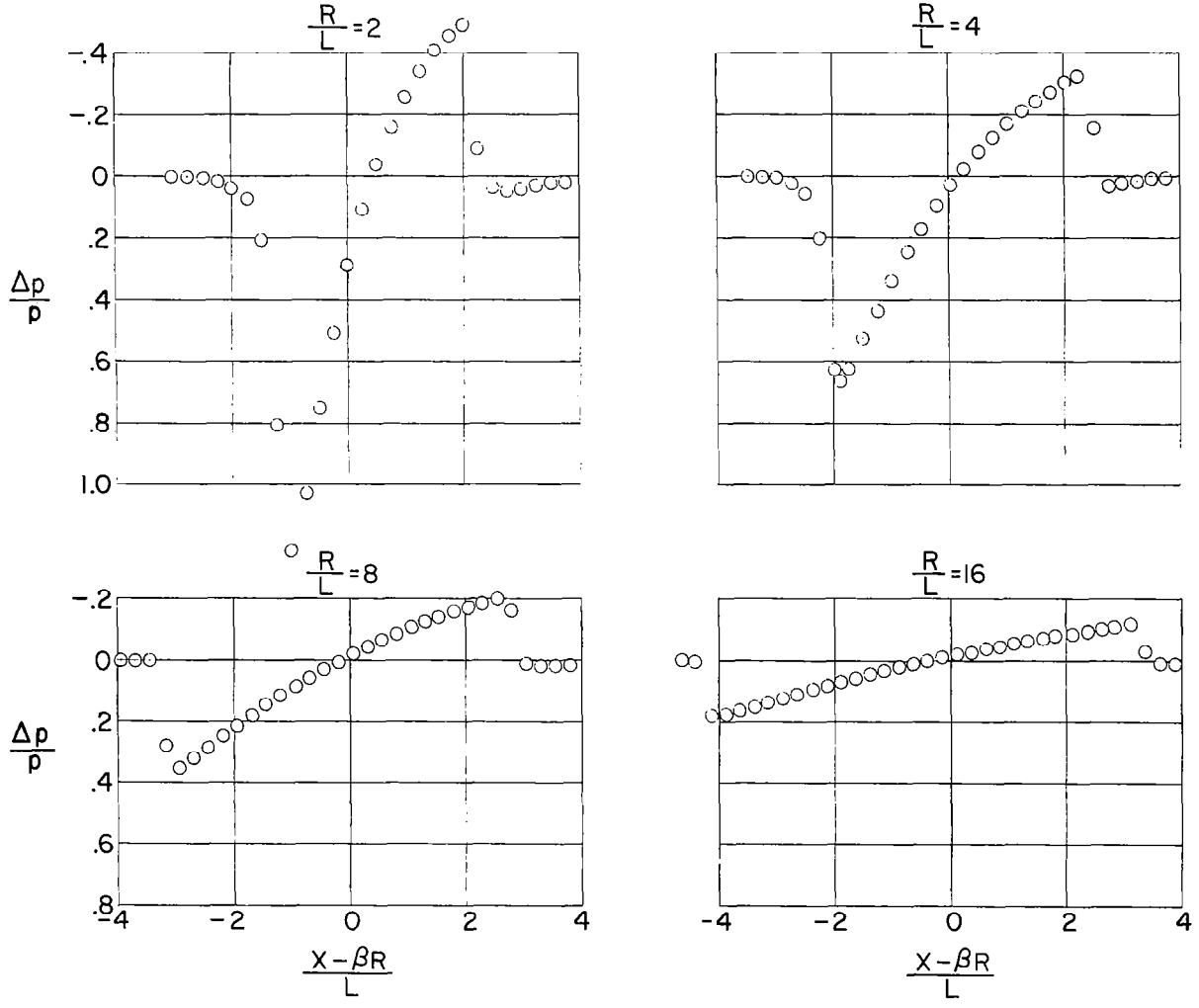

(g) $\alpha = 10^{\circ}$; $\phi = 0^{\circ}$.

Figure 9.- Continued.

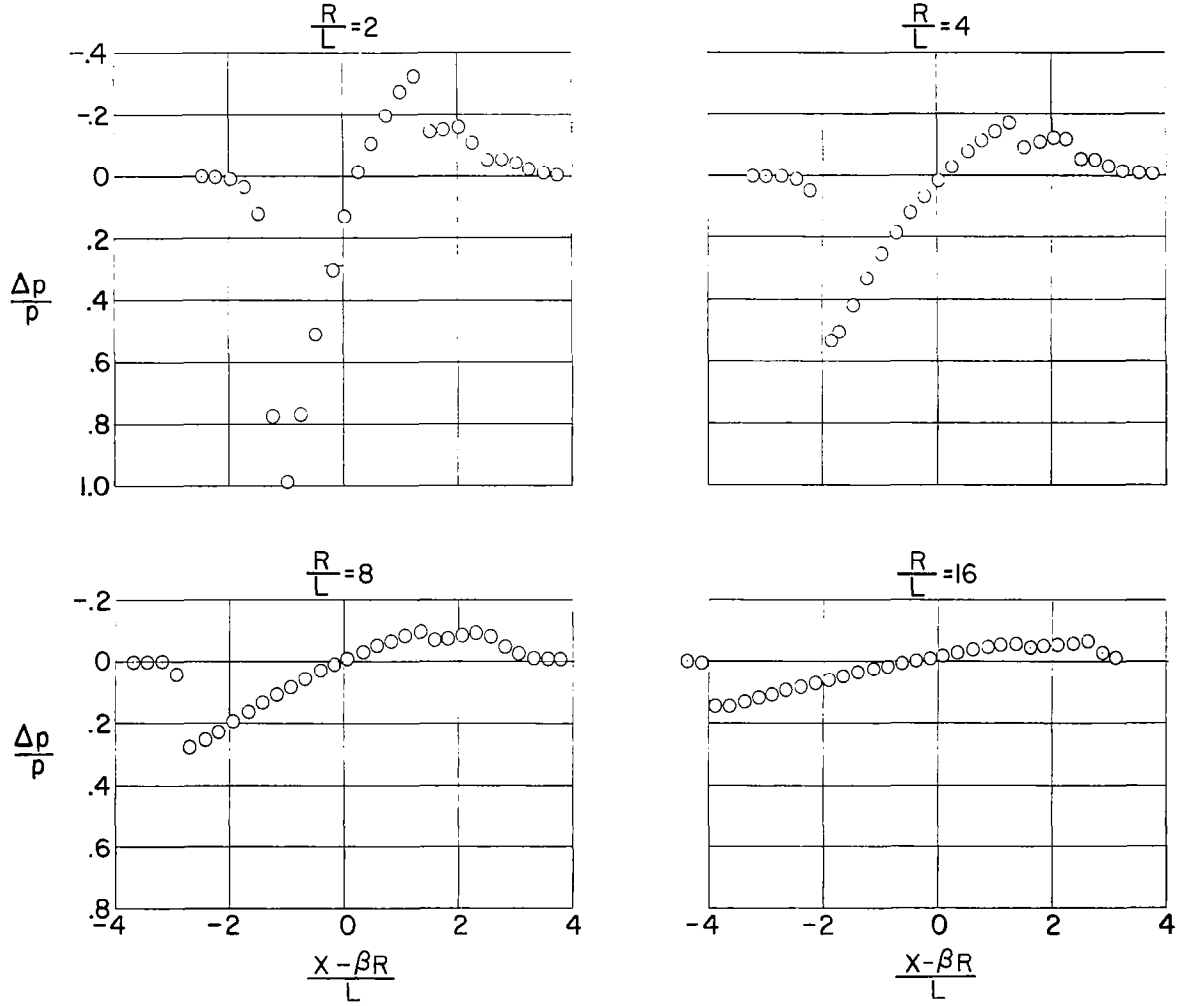

(h) $\alpha = 10^{\circ}$; $\phi = 45^{\circ}$.

Figure 9.- Continued.

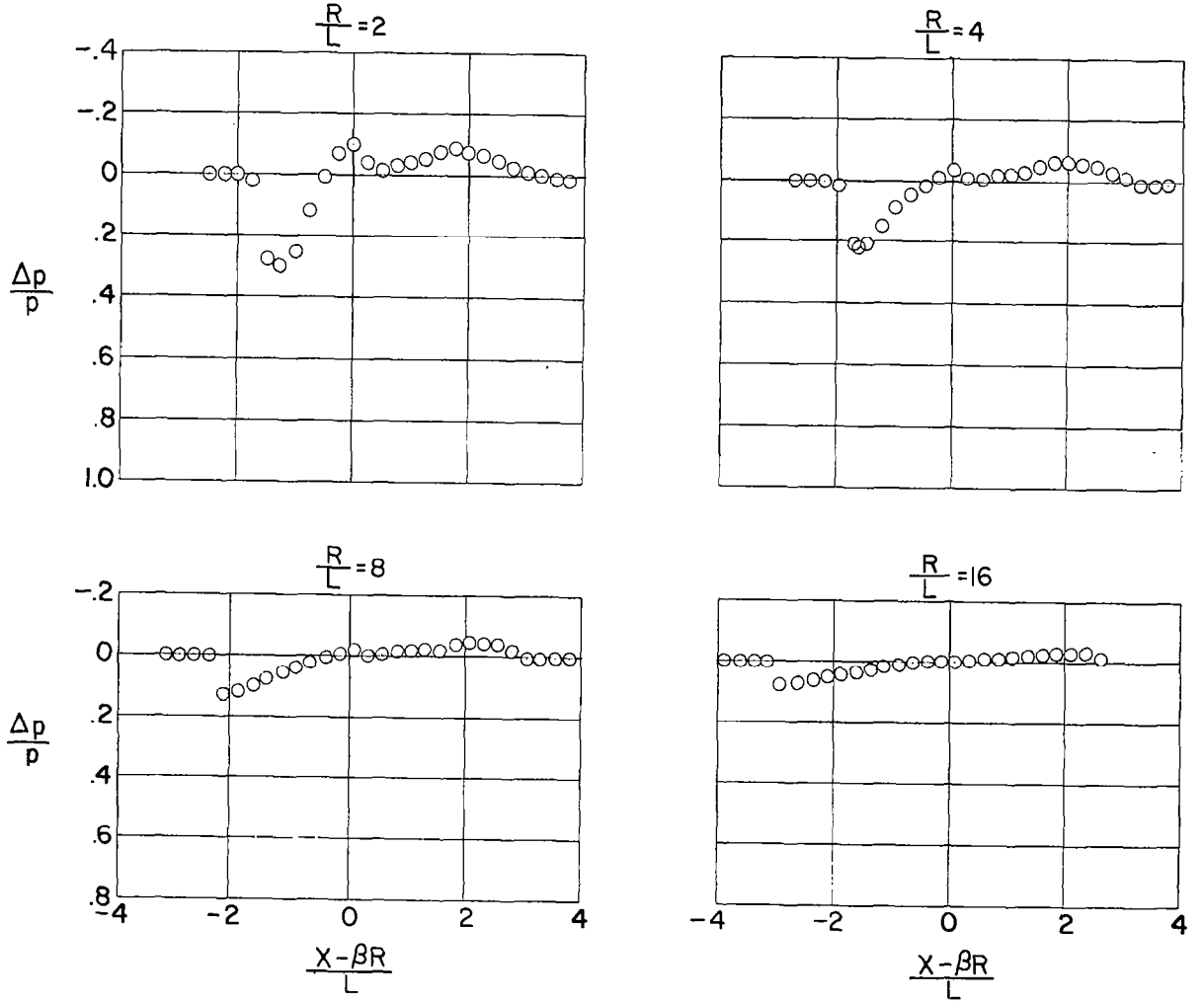

(i) $\alpha = 10^{\circ}$; $\phi = 90^{\circ}$.

Figure 9.- Continued.

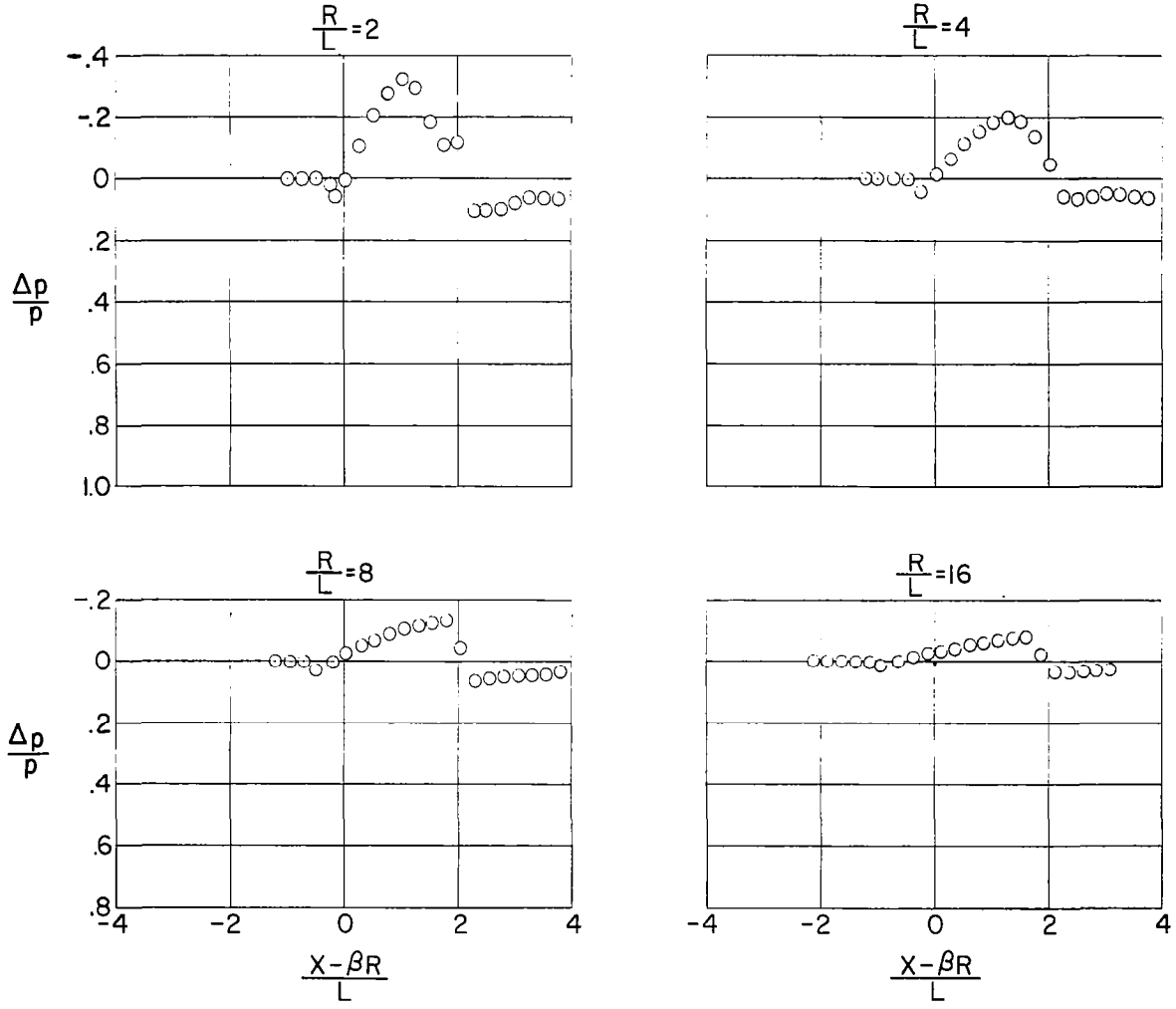

(j) $\alpha = 10^{\circ}$; $\phi = 180^{\circ}$.

Figure 9.- Concluded.

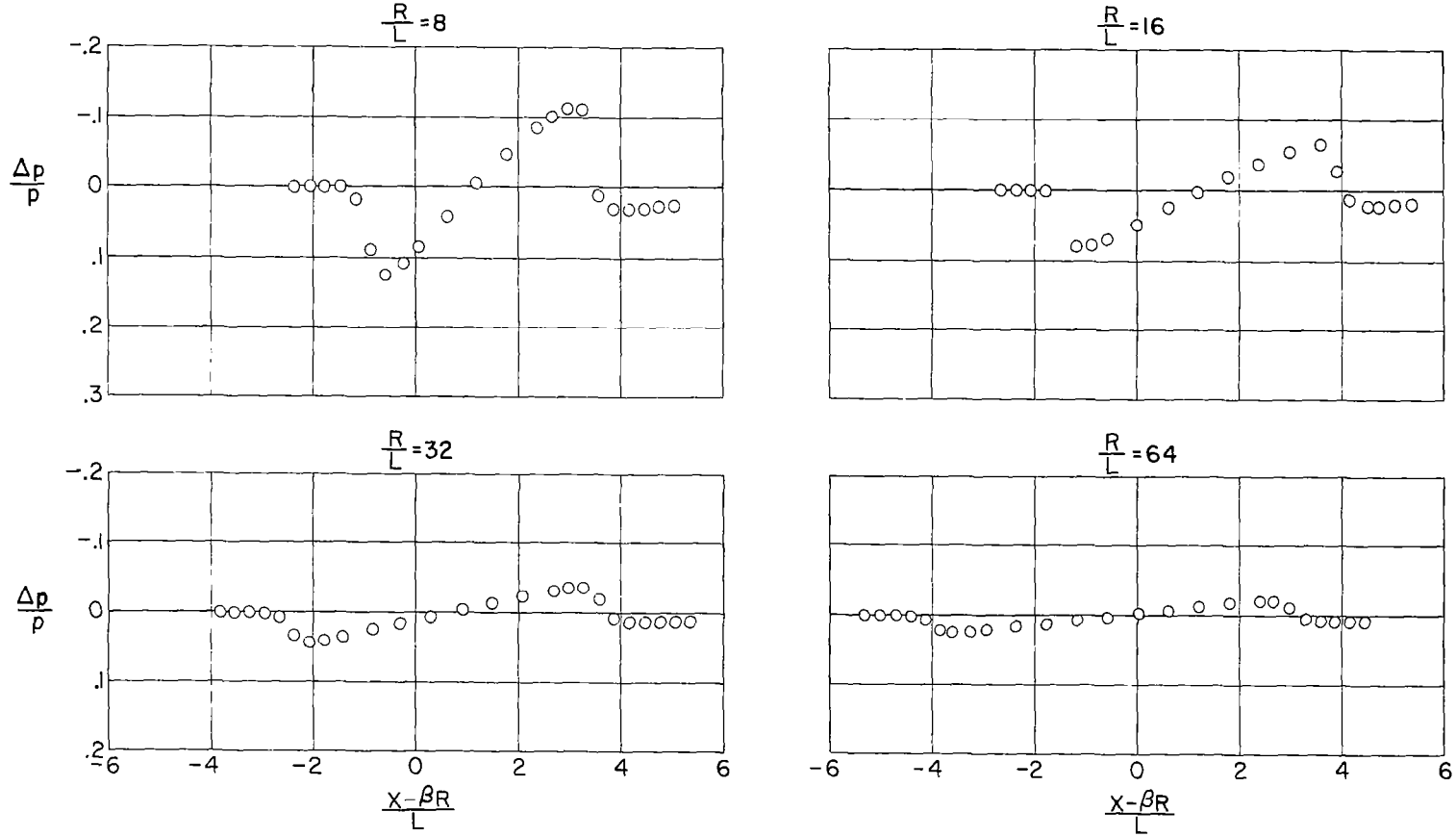

(a) $\alpha = 0^{\circ}$; $\phi = 0^{\circ}$.

Figure 10.- Pressure ratio measured on the surface of the boundary-layer bypass plate. Model F.

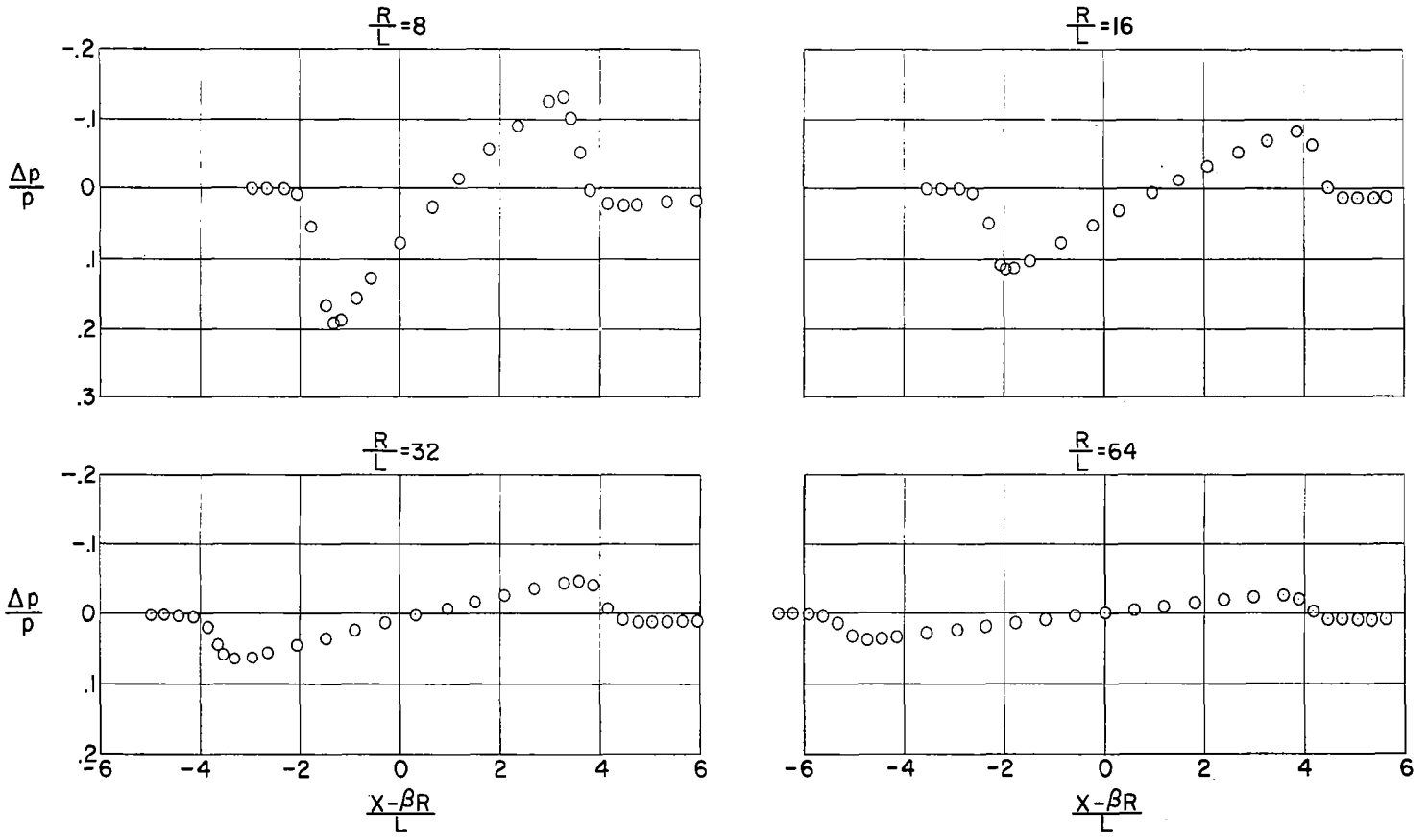

(b) $\alpha = 5^{o}$; $\phi = 0^{o}$.

Figure 10.- Continued.

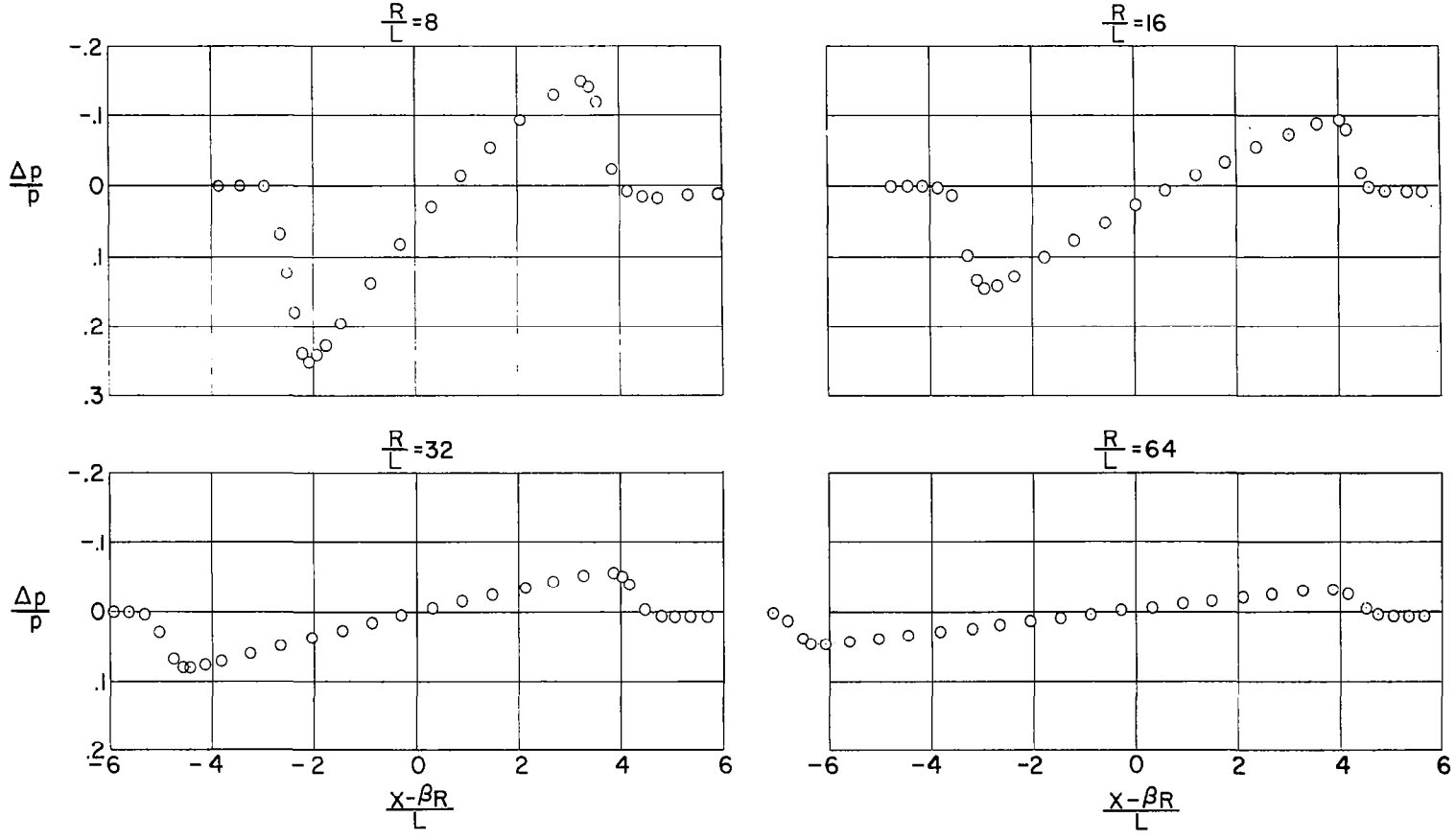

(c) $\alpha = 10^{\circ}$; $\phi = 0^{\circ}$.

Figure 10.- Concluded.

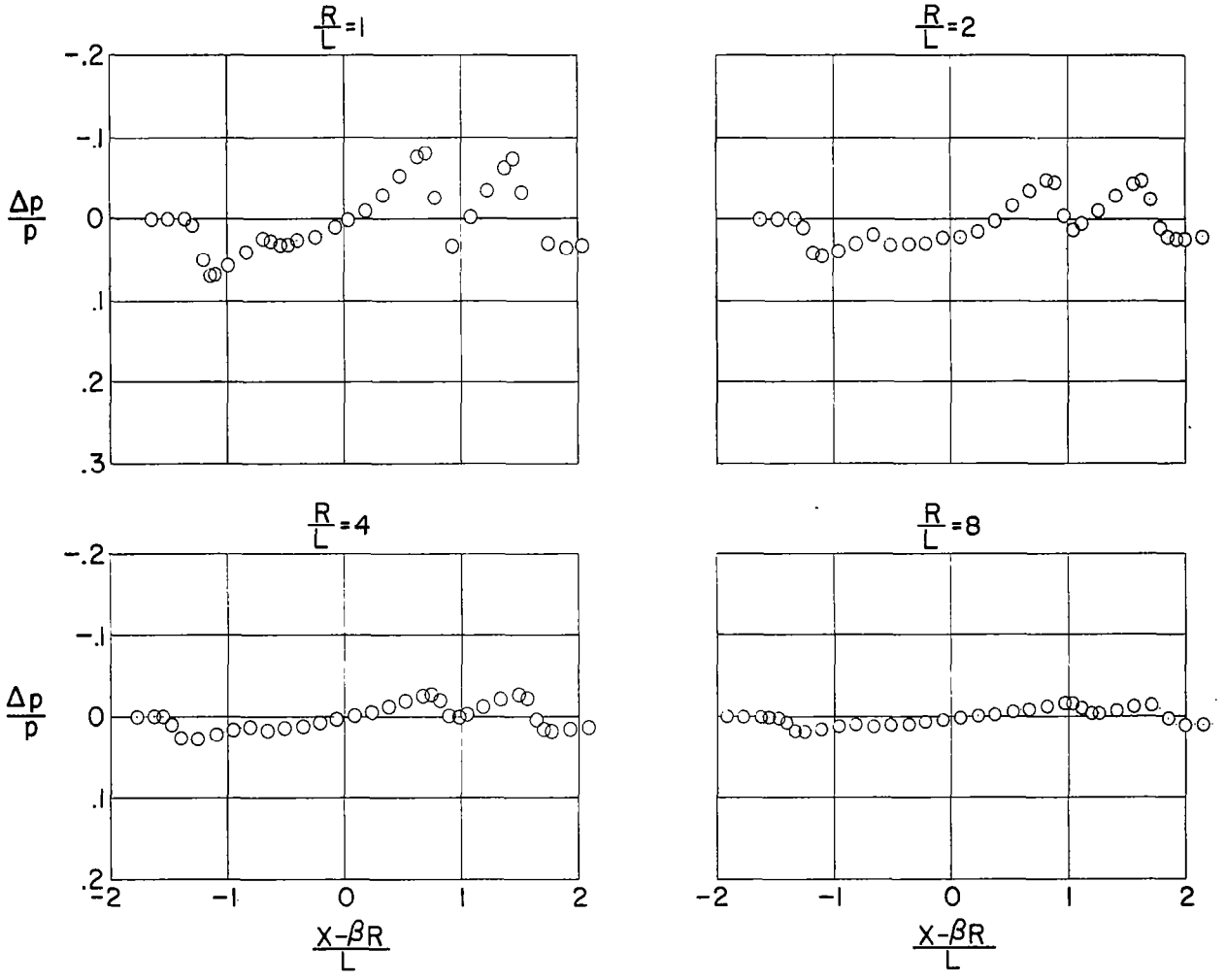

(a) $\alpha = 0^{o}$; $\phi = 0^{o}$.

Figure 11.- Pressure ratio measured on the surface of the boundary-layer bypass plate. Model G.

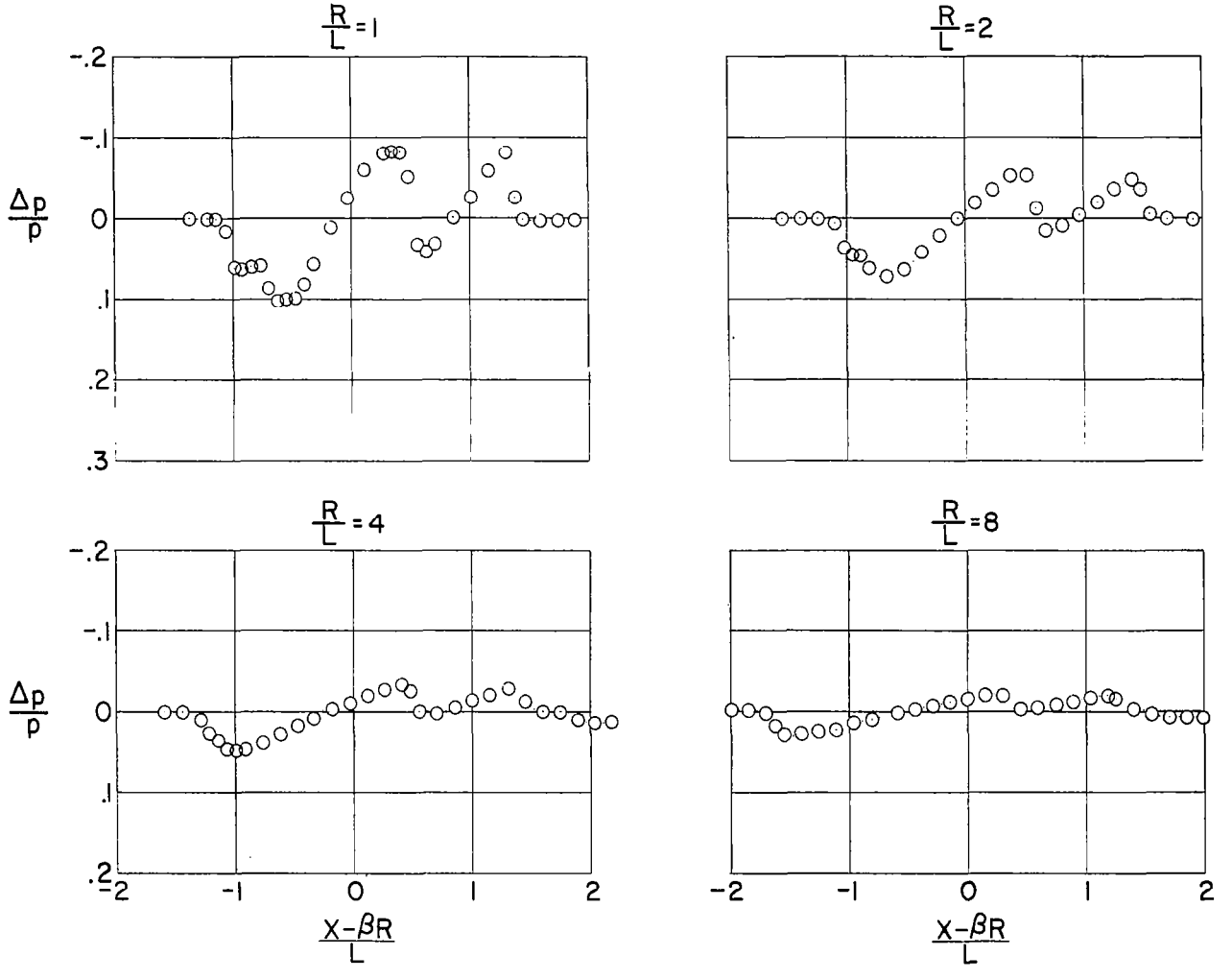

(b) $\alpha = 0^{\circ}$; $\phi = 90^{\circ}$.

Figure 11.- Continued.

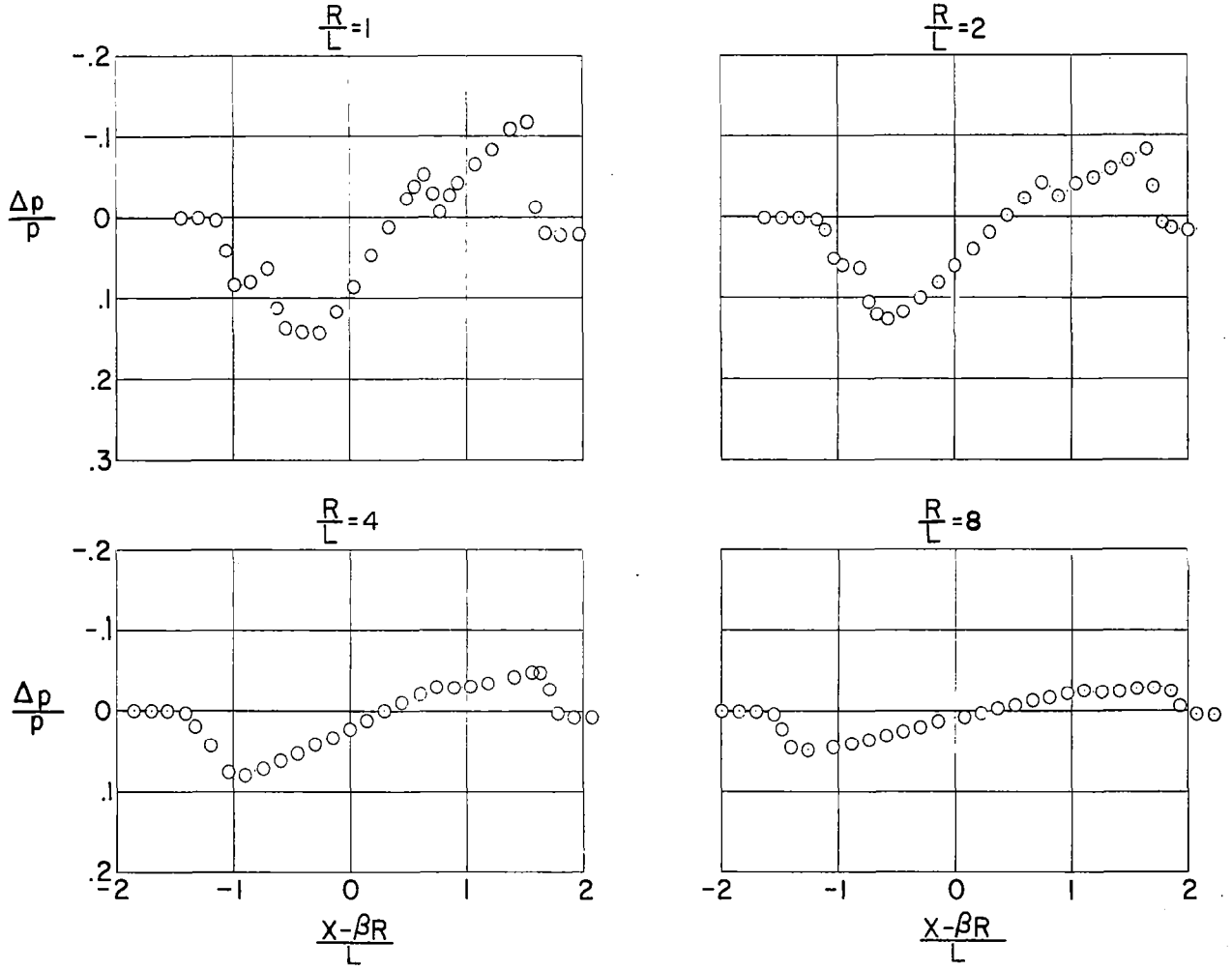

(c) $\alpha = 5^{\circ}$; $\phi = 0^{\circ}$.

Figure 11.- Concluded.

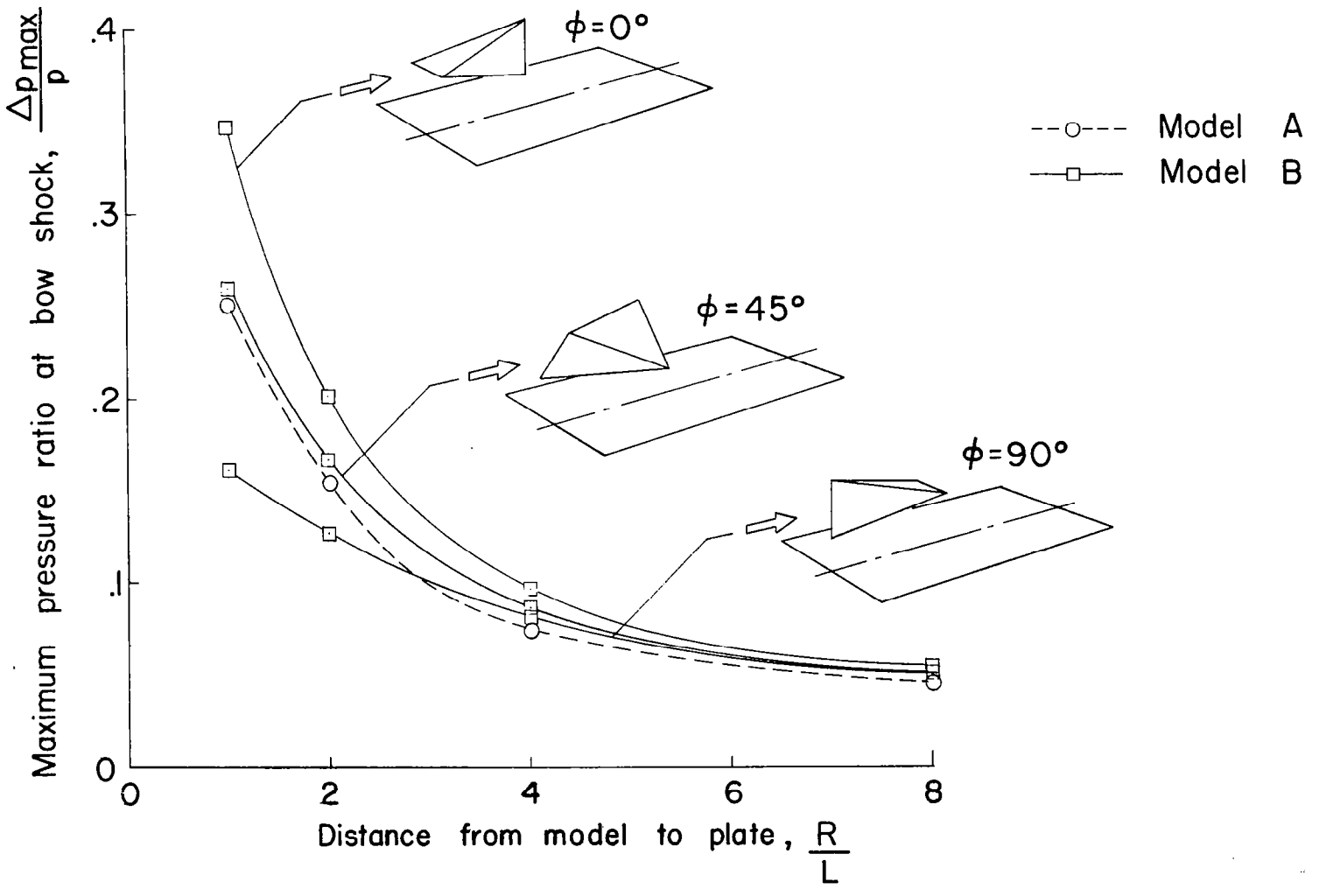

Figure 12.- Attenuation with distance of pressure rise at the bow shock for several orientations of model B and a comparison with data for model A.

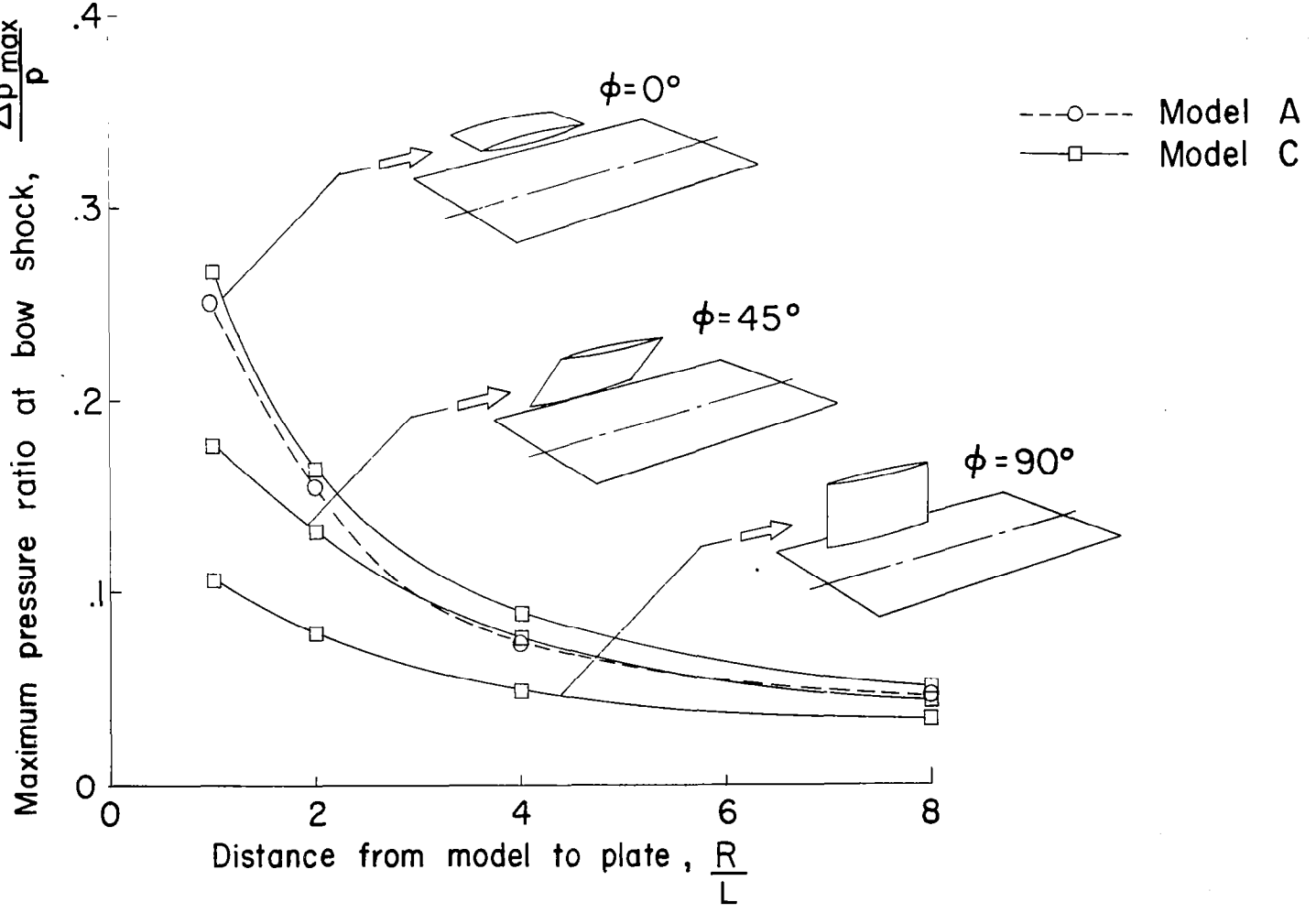

Figure 13.- Attenuation with distance of pressure rise at the bow shock for several orientations of model C and comparison with data for model A.

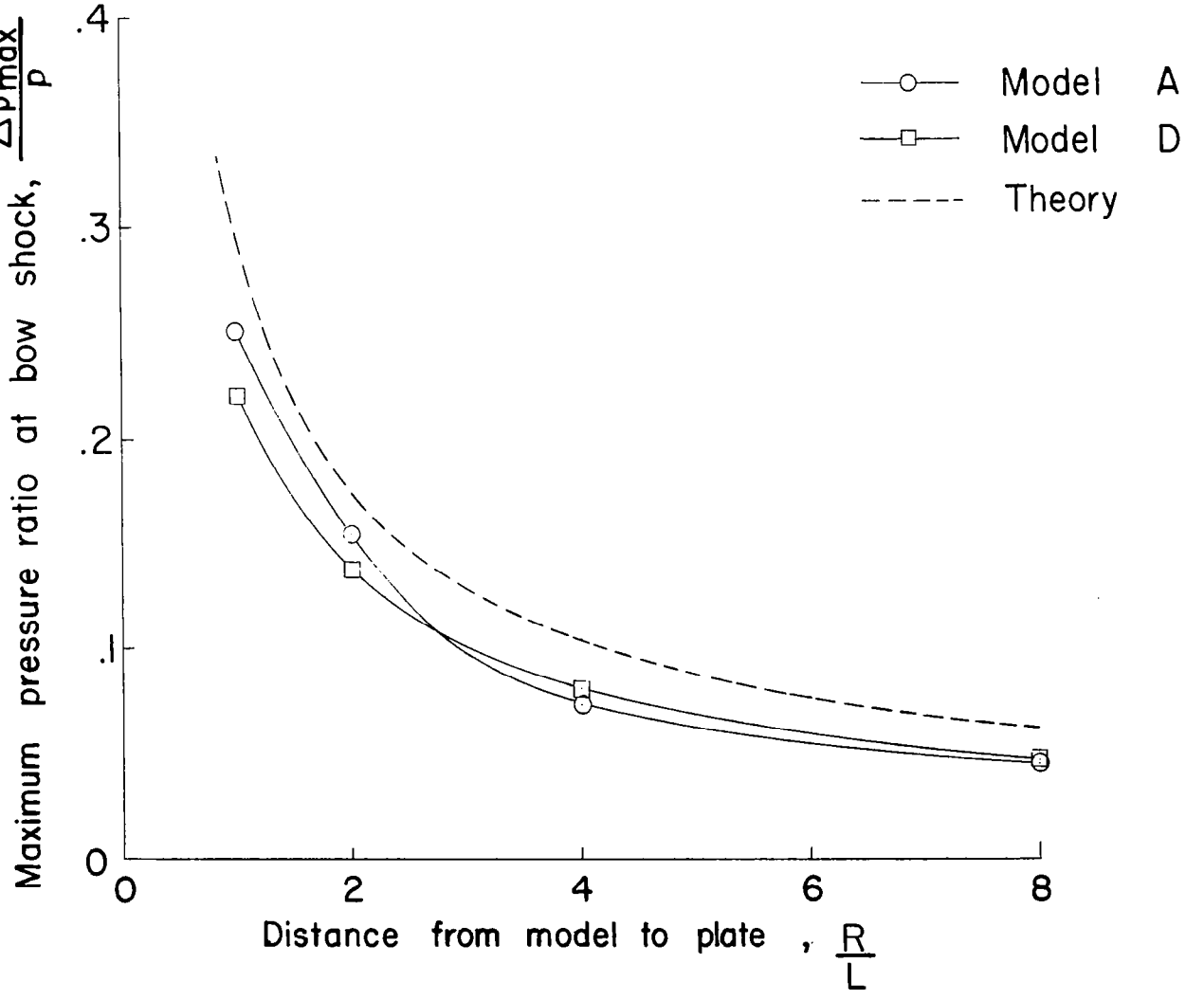

Figure 14.- Comparison of theoretical and experimental attenuation of pressure rise at the bow shock for bodies of revolution. Models A and D.

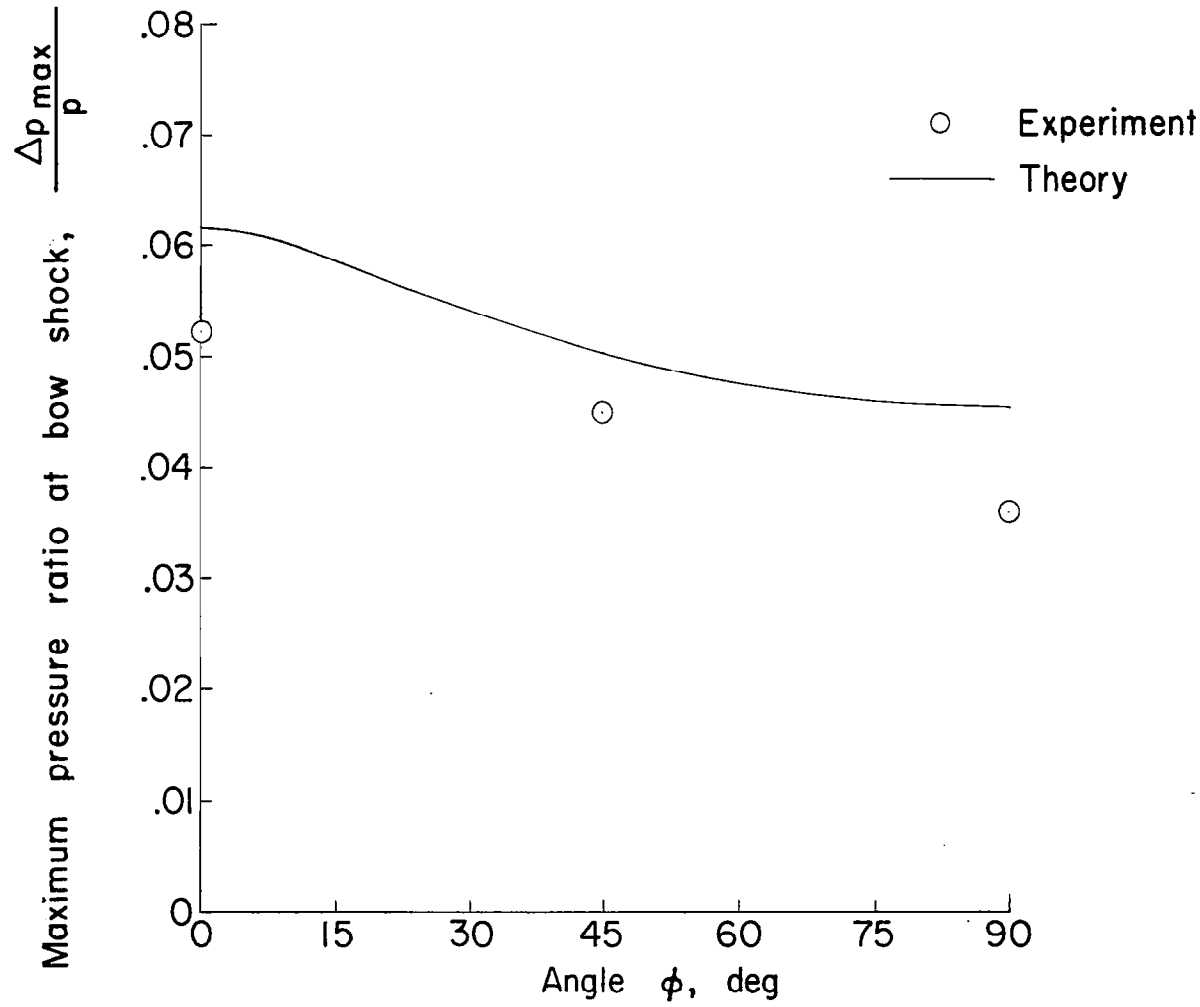

Figure 15.- Comparison of theoretical and experimental variation of pressure rise with radial position. Model C; $\frac{R}{L} = 8$.

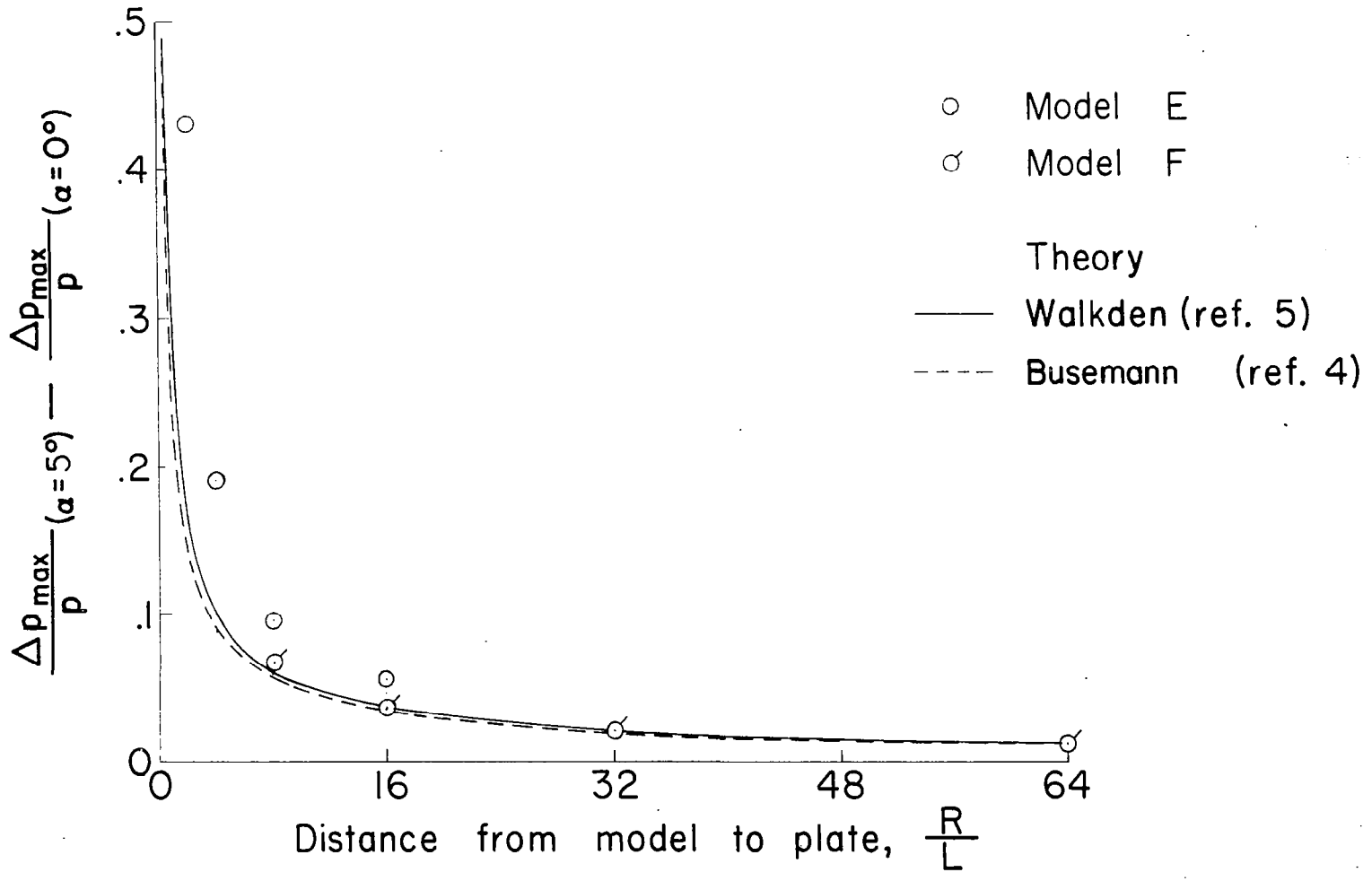

Figure 16.- Comparison of theoretical and experimental attenuation of lift-induced pressure rise at the bow shock for models E and F. $\phi = 0^{\circ}$.

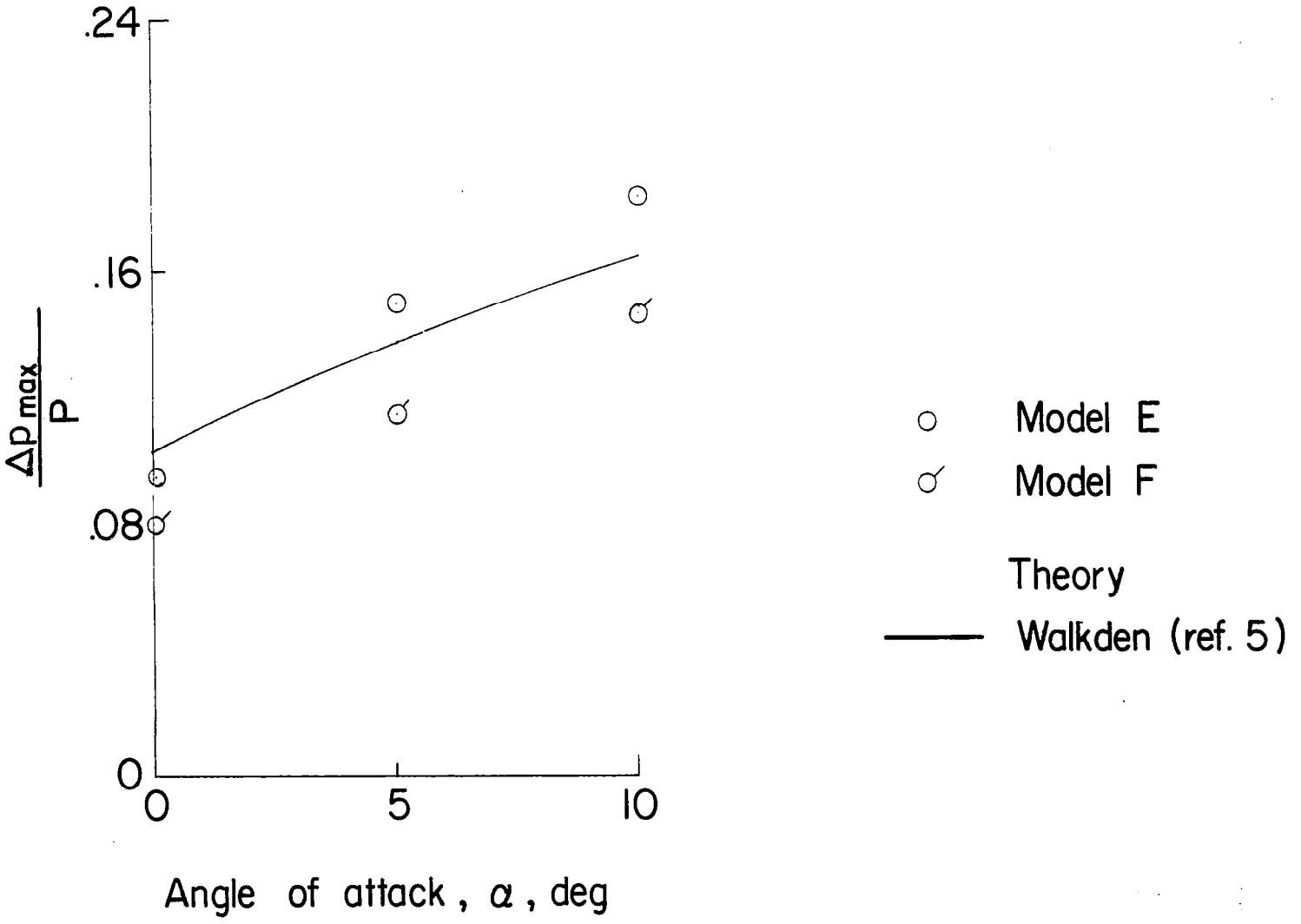

Figure 17.- Comparison of theoretical and experimental variation of pressure rise at the bow shock with angle of attack. Models E and F; $\frac{R}{L} = 16$; $\phi = 0^{\circ}$.

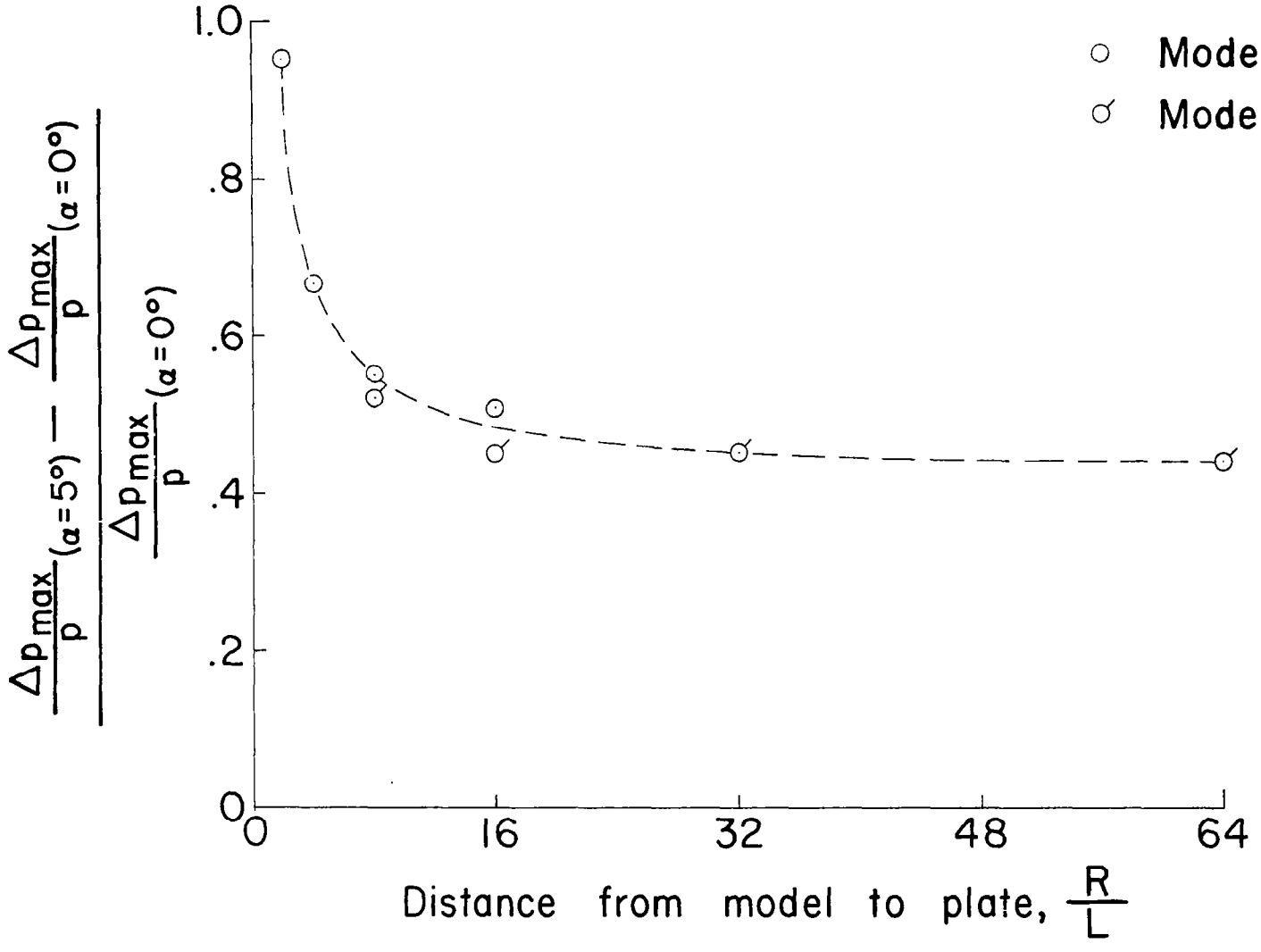

Figure 18.- Ratio of lift-induced to thickness-induced pressure rise as a function of distance. Models E and F; $\phi = 0°$.